ARTICLE
Journal of Cellular Biochemistry 117:180–196 (2016)

Journal of Cellular Biochemistry

Regulation of Adipose Tissue Stem Cells Angiogenic Potential by Tumor Necrosis Factor-Alpha

Ekaterina S. Zubkova,[1] Irina B. Beloglazova,[1]* Pavel I. Makarevich,[1,2] Maria A. Boldyreva,[1] Olga Yu. Sukhareva,[3] Marina V. Shestakova,[3,4] Konstantin V. Dergilev,[1] Yelena V. Parfyonova,[1,2] and Mikhail Yu. Menshikov[1]

[1]*Russian Cardiology Research and Production Complex, Moscow, Russian Federation*
[2]*Faculty of Medicine, Lomonosov Moscow State University, Moscow, Russian Federation*
[3]*Endocrinology Research Centre, Moscow, Russian Federation*
[4]*I.M. Sechenov First Moscow State Medical University, Moscow, Russian Federation*

ABSTRACT

Tissue regeneration requires coordinated "teamwork" of growth factors, proteases, progenitor and immune cells producing inflammatory cytokines. Mesenchymal stem cells (MSC) might play a pivotal role by substituting cells or by secretion of growth factors or cytokines, and attraction of progenitor and inflammatory cells, which participate in initial stages of tissue repair. Due to obvious impact of inflammation on regeneration it seems promising to explore whether inflammatory factors could influence proangiogenic abilities of MSC. In this study we investigated effects of TNF-α on activity of adipose-derived stem cells (ADSC). We found that treatment with TNF-α enhances ADSC proliferation, F-actin microfilament assembly, increases cell motility and migration through extracellular matrix. Exposure of ADSC to TNF-α led to increased mRNA expression of proangiogenic factors (FGF-2, VEGF, IL-8, and MCP-1), inflammatory cytokines (IL-1β, IL-6), proteases (MMPs, uPA) and adhesion molecule ICAM-1. At the protein level, VEGF, IL-8, MCP-1, and ICAM-1 production was also up-regulated. Pre-incubation of ADSC with TNF-α-enhanced adhesion of monocytes to ADSC but suppressed adherence of ADSC to endothelial cells (HUVEC). Stimulation with TNF-α triggers ROS generation and activates a number of key intracellular signaling mediators known to positively regulate angiogenesis (Akt, small GTPase Rac1, ERK1/2, and p38 MAP-kinases). Pre-treatment with TNF-α-enhanced ADSC ability to promote growth of microvessels in a fibrin gel assay and accelerate blood flow recovery, which was accompanied by increased arteriole density and reduction of necrosis in mouse hind limb ischemia model. These findings indicate that TNF-α plays a role in activation of ADSC angiogenic and regenerative potential. J. Cell. Biochem. 117: 180–196, 2016.

KEY WORDS: ADIPOSE-DERIVED STEM CELL; TNF-α; ANGIOGENESIS; INFLAMMATION; REGENERATION

Regeneration of damaged tissue is a complex process stimulated by a variety of factors and cell types, including mesenchymal stem cells (MSC), which are known to play significant role in successful restoration of tissue morphology and function [Nesselmann et al., 2008].

In adults MSC have been isolated from nearly every organ from bone marrow to adipose tissue [da Silva Meirelles et al., 2006]. It is suggested that they reside in a perivascular niche—a specialized environment that maintains MSC self-renewal and prevents them from differentiating. In these steady-state conditions MSC are probably quiescent most of the time, but under certain stimuli they can be mobilized to facilitate tissue regeneration [Jones and Wagers, 2008]. One of these stimuli is probably inflammation, which accompanies any tissue lesion and is a natural response to damage or infection [Singer and Clark, 1999]. During injury and early phases of regeneration, plenty of pro-inflammatory factors is released by resident or by immune cells attracted to the site of injury. [Coussens and Werb, 2002]. These paracrine effects may play a role in activation of MSC-driven tissue repair and angiogenesis in adult tissues.

Among a broad spectrum of inflammatory factors TNF-α is of particular interest from this point of view. In the early course of

Conflict of Interest: None.

Grant sponsor: Russian Federation Ministry of Health (subsidy #01113 of 12.11.2013); Grant sponsor: RFBR; Grant number: 12-04-00989.

*Correspondence to: Irina Borisovna Beloglazova, Laboratory of Angiogenesis, Russian Cardiology Research and Production Complex, 3-rd Cherepkovskaya 15a, Moscow, 121552, Russian Federation.
E-mail: irene.beloglazova@gmail.com; irene@cardio.ru

Manuscript Received: 28 October 2014; Manuscript Accepted: 16 June 2015

Accepted manuscript online in Wiley Online Library (wileyonlinelibrary.com): 20 June 2015

DOI 10.1002/jcb.25263 • © 2015 Wiley Periodicals, Inc.

tissue damage it is predominantly produced by monocytes and its committed lineage—macrophages, but also by lymphoid, mast cells, endothelium, fibroblasts, and neural cells. TNF-α drives inflammatory response and may play a role in tissue repair for instance due to enhancement of MSC homing, which was observed after TNF-α treatment [Xiao et al., 2012]. All above-mentioned allows to suggest that TNF-α may be the trigger that activates MSC's "exodus" from the niche and recruits them into regenerative process. Furthermore, in MSC TNF-α up-regulates production of pro-angiogneic and pro-survival growth factors including VEGF, FGF-2, and HGF [Crisostomo et al., 2008; Lee et al., 2010].

From a variety of MSCs adipose-derived stromal cells (ADSC) are known for feasible isolation, expansion and can be applied for therapeutic development [Bertassoli et al., 2013]. Compared to bone marrow aspiration grafting of ADSC by needle or liposuction is less painful and more appropriate for patient use (including autologous approaches).

A number of studies including our own indicates that transplantation of ADSC increases vascularization and stimulates regeneration in ischemic tissue [Shevchenko et al., 2013]. This probably involves a number of mechanisms, which result in a combined mode of action of ADSC where replacement of injured cells and paracrine action seem to be the key factors. In addition, ADSC possess a pericyte-like phenotype and function, which may play role in blood vessel maturation and remodeling [Merfeld-Clauss et al., 2010; Rohringer et al., 2014]. Overall we assume that intrinsic regenerative abilities of ADSC can be activated by inflammatory cytokines and TNF-α may be of particular importance as a key mediator of inflammatory response after injury.

Here, we studied influence of TNF-α on ADSC proliferation, migration, expression profile, and interaction with endothelial cells or monocytes in vitro and assessed its impact on ADSC's ability to stimulate regeneration and angiogenesis in vivo in mouse hind limb ischemia model.

MATERIALS AND METHODS

CELL ISOLATION AND CULTURE

Human ADSC were isolated from subcutaneous adipose tissue harvested during surgery from patients of 21–55 years of age (predominantly males); all donors provided informed consent for tissue sampling. Subjects with infectious, systemic diseases or malignancies were not included in the study. Tissue samples were minced and digested in collagenase I solution (200 U/ml) (Sigma-Aldrich, USA) under gentle agitation for 1 h at 37°C, centrifuged (200g, 10 min) to separate the stromal-vascular cell fraction from mature adipocytes. The supernatant was discarded, pelleted stromal cells were resuspended and passed through a 40 μm cell strainer before plating. Isolated cells were cultured in the complete AdvanceSTEM™ medium (Thermo Scientific HyClone, USA) at 5% CO_2, 37°C. Mouse ADSC were isolated from subcutaneous adipose tissue of adult male C57Bl6 mice using similar procedure. Human umbilical vein endothelial cells (HUVEC) were obtained from the ATCC and cultured in complete EGM-2 medium (Lonza, USA) until 3–5 passage. All cells were maintained in a humidified chamber at 37°C and 5% CO_2. THP-1 monocytic cell line was purchased from ATCC and cultured in RPMI-1640 /10% fetal bovine serum (Life Technologies, USA).

FLOW CYTOMETRY AND CELL CYCLE ANALYSIS

To analyze expression of surface antigens human ADSC were stained by specific antibodies (Ab). Antigen expression was analyzed using flow cytometer FACS Canto™ II (BD Pharmingen, USA). Apoptotic cells prevalence in ADSC was assessed after overnight treatment with TNF-α using FITC Annexin V Apoptosis Detection Kit II (BD Bioscience, USA). To evaluate cell cycle distribution ADSC were incubated for 48 h with TNF-α (5 ng/ml), after that cells were detached and fixed with ice-cold 70% ethanol for 4 h. After denaturation of DNA with 2 N HCl/0.5% Triton X-100 (RT, 30 min) acidic solution was neutralized with 0.1 M borate buffer (pH 8.5). Cells were washed and resuspended in propidium iodide (Life Technologies, USA) solution (50 μg/ml). Stained cells were analyzed by flow cytometry using cytometer BD FACS Canto™ II (BD Pharmingen, USA). FCS Express 4 software (De Novo Software, Canada) was used for analysis of cell distribution over cell cycle stages basing on the intensity of propidium iodide fluorescence.

CELL VIABILITY AND PROLIFERATION ASSESSMENT

Cell viability was evaluated by manual counts with trypan blue exclusion stain and by MTT assay developed by Mosmann [Mosmann, 1983]. ADSC were plated in 96-well culture plates (5×10^3 cells/well) in DMEM/5% FBS in a final volume of 0.1 ml. Standard calibration curves (absorbance against number of cells) were plotted using 6 serial dilutions from 620 to 20000 cells/well. After 4 h. culture medium was replaced with DMEM/1% FBS containing TNF-α at 0, 5, and 100 ng/ml with or without following substances: (1) ROS scavenger TIRON-4,5 (dihydroxy-1,3-benzene-disulfonic acid) at final concentration of 3mM; (2) PI3K inhibitor LY294002 at 1 μM; 3) corresponding solvent control. Cells were incubated for 24, 48, 72, or 96 h and then 20 μl of 3-(4.5-dimethylthiazol-2-yl)-2.5-diphenyltetrazolium bromide (stock 2.5 mg/ml) was added to the culture medium for another 4 h. Formazan crystals were solubilized by adding 0.1 N HCl in isopropanol. Absorbance was measured at 595 nm (reference filter 620 nm) using Multiscan Microplate Reader (Labsystems, USA) and number of cells per well was calculated using plotted standard curve.

IMMUNOFLUORESCENT STAINING AND VESSEL DENSITY ANALYSIS

ADSC grown on glass coverslips were incubated overnight with TNF-α (0, 5, or 100 ng/ml), fixed, permeabilized, stained with primary Ab against Ki-67, vinculin or isotype-matched controls and subsequently with fluorofore-labeled secondary Ab and Alexa Fluor® 594-conjugated phalloidin.

Frozen sections of *m. tibialis anterior* were immunostained with Ab against CD31 and α-smooth muscle actin (α-SMA) and then with suitable secondary Ab. Immunofluorescence was visualized using an Axiovert 200M inverted microscope, equipped with an AxioCam HR digital camera (Carl Zeiss, Germany). CD31+ capillaries and α-SMA+ arterioles were counted manually per FOV in images acquired. Detailed staining procedure can be found in online Supplementary materials.

IN VITRO "WOUND HEALING" ASSAY

ADSC at passage 2-3 were allowed to grow to form confluent monolayer in a 24-well plate. Cell monolayers were scratched twice with a 1 ml pipette tip. Dislodged cells were washed out with DPBS and serum-free medium containing 5 or 100 ng/ml TNF-α alone or in combinations with either recombinant human PDGF-BB (10 ng/ml) or EGF (10 ng/ml) or SDF-1α (150 ng/ml) (all from R&D Systems, USA) were added. Individual controls (without TNF-α) were run in parallel for each factor. Cells in selected wells of 24-well plate were cultured in presence of TNF-α (5 ng/ml) overnight prior to experiment ("pre-T5"). Images of scratched wells were acquired at 0 and 18 h after chemoattractant addition. "Wound healing" was determined by measurement of unfilled area in each field of view (FOV) using ImageJ software.

TRASNWELL MIGRATION ASSAY

Migration assay was performed as described previously [Zubkova et al., 2012]. Briefly, ADSC were deprived in a serum-free medium for 18 h, then detached and resuspended in assay medium (DMEM/0.25% BSA) and in some experiments pretreated with 20 μM ebselen or solvent control for 1 h at 37°C, 5% CO_2. Cell suspension (10^5/well) in presence or absence of TNF-α (5 ng/ml) was placed in the inserts of a 24-well Transwell system (Corning Inc., USA). Filters (8 μm pore size) were preliminary coated with 100 μg/ml of rat type I collagen solution (Imtek, Russia). Assay medium, TNF-α (5 ng/ml) or RANTES/CCL5 (150 ng/ml) were placed in lower chambers and served as chemoattractants. After 24 h incubation, migrated cells were stained (Diff-Quick Differential Staining Set, Dade Behring–Siemens Healthcare Diagnostics Inc., USA), photographed, and counted in at least five randomly selected FOV using ImageJ software.

Invasion assay was performed using filters coated with growth factor-reduced Matrigel™ (Corning Inc., USA) diluted 1:3 with DMEM medium. ADSC (10^5 per well) were seeded into the upper chamber, 15% FBS or TNF-α (5 ng/ml) were added to the bottom well as chemoattractants. After 48 h of incubation filters were processed as described above.

RNA ISOLATION, REVERSE TRANSCRIPTION AND REAL-TIME QUANTITATIVE PCR

Total RNA was isolated using RNeasy Mini Kit (QIAGEN, USA). First strand cDNA was synthesized with oligo(dT)-primer using RevertAid™ First Strand cDNA Synthesis Kit (Fermentas, Latvia). PCR was performed with SYBR Green intercalating dye (Syntol, Russia) in StepOnePlus™ Real-Time PCR System (Applied Biosystems, USA); primers used for PCR are listed in Table I. Reaction mixture (25 μl) contained 1–5 ng of cDNA, 10 pmol of each primer, 10 μl of dNTP/polymerase solution (Sintol, Russia) and deionized water up to 25 μl. Control mixture contained all components except matrix (replaced by deionized water). After the initial stage of denaturation (95°C, 10 min), 40 amplification cycles with annealing/elongation at 60°C, 60 s were performed for all primer pairs. Specificity of amplification was analyzed by melting stage upon PCR completion and by electrophoresis of amplicons in agarose gel.

ENZYME-LINKED IMMUNOSORBENT ASSAY (ELISA)

ADSC were cultured in 24-well culture plates at 70×10^3 cells/well density with TNF-α (0, 5, or 100 ng/ml) for 24 or 48 h. At endpoint culture medium samples were collected, centrifuged and stored at −20°C until assayed. Concentration of VEGF165 was assayed using Human VEGF Quantikine ELISA Kit (R&D Systems, USA); concentration of MCP-1 or IL-8 was measured using OptEIA™ MCP-1 ELISA Set or IL-8 ELISA Set (BD Biosciences, USA) respectively. Optical densities in 96-well plates were read using Victor™ X3 Multilabel Plate Reader (Perkin-Elmer Inc., USA).

TABLE I. Primers Used for Semi-Quantitative PCR

cDNA	Sense primer	Anti-sense primer
ACTB	5′-cctggcacccagcacaat-3′	5′-gggccggactcgtcatac-3′
ANGPT1	5′-ctcgctgccattctgactcac-3′	5′-gacagttgccatcgtgttctg-3′
FGF-2	5′-aagcggctgtactgcaaaaac-3′	5′-tgagggtcgctcttctccc-3′
GAPDH	5′-tgcaccaccaactgcttagc-3′	5′-ggcatggactgtggtcatgag-3′
ICAM-1	5′-attcaaactgccctgatggg-3′	5′-ggtaaggttcttgcccactg-3′
Il-1β	5′-acagatgaagtgctccttcca-3′	5′-gtcggagattcgtagctggat-3′
Il-4	5′-agaagactctgtgcaccgagttga-3′	5′-ctctcatgatcgtctttagcctttt-3′
Il-6	5′-tcaatgaggagacttgcctg-3′	5′-gatgagttgtcatgtcctgc-3′
Il-8	5′-ctggccgtggctctcttg-3′	5′-ccttggcaaaactgcacctt-3′
Leptin	5′-ttcattgccaaaagagtcacct-3′	5′-acacgagcaagaataacaggaaa-3′
MMP-2	5′-ccgtcgcccatcatcaagtt-3′	5′-ctgtctggggcagtccaaag-3′
MMP-9	5′-gggacgcagacatcgtcatc-3′	5′-tcgtcatcgtcgaaatgggc-3′
PAI-1	5′-catcccccatcctacgtgg-3′	5′-ccccatagggtgagaaaacca-3′
PPAR-γ	5′-tctctccgtaatggaagacc-3′	5′-gcattatgagacatccccac-3′
TGF-β	5′-caagcagagtacacacagcat-3′	5′-tgctccacttttaacttgagcc-3′
uPA	5′-tcaaaaacctgctatgagggga-3′	5′-gggcatggtacgtttgctg-3′
uPAR	5′-tattcccgaagccgttacctc-3′	5′-ggtggcggtcatcctttgg-3′
VCAM-1	5′-ataatgggaatctacagcacct-3′	5′-aacatgactgagtctccaatctg-3′
VEGF	5′-caacatcaccatgcagattatgc-3′	5′-gctttcgtttttgcccctttc-3′

CELL ATTACHMENT ASSAY

Prior to test HUVEC at passage 3–4 were seeded on a 24-well plate and grown till they form a confluent monolayer. Test was performed using THP-1 monocytic cell line and human ADSC at passage 3-4 and 70–80% confluence, pre-treated by TNF-α (0 or 5 ng/ml) in complete medium overnight. ADSC were labeled with 5 μM of CellTracker™ Green CMFDA (Life Technologies, USA) and THP-1 cells were labeled with 2 μM PKH26 (Sigma-Aldrich, USA). The following cell suspensions were prepared in 0.5 ml of warm DMEM gassed with 5% CO_2: (1) TNF-α–treated ADSC (5×10^4/500 μl) alone or (2) mixed with PKH-labeled THP-1 (1×10^5/500 μl); (3) untreated ADSC alone or (4) mixed with THP-1 as described above. Liquid from wells with HUVEC monolayer was aspirated and 500 μl of prepared suspensions were loaded onto each well. Plates were incubated at 37°C with lid off for 40 min or 2 h in CO_2 incubator. After incubation nonadherent cells were removed by gentle washing three times with PBS. Attached cells were fixed in 4% paraformaldehyde and photographed using a fluorescent inverted microscope Axiovert 200-M (five random FOV at 10×magnification). In separate experiments ADSC were grown to confluence and stimulated overnight with 0, 5 or 100 ng/ml of TNF-α in complete medium. After that, culture medium was aspirated and 1×10^5/500 μl of PKH26-labeled THP-1 cells were loaded onto each well. All further stages were processed as described above.

WESTERN BLOT ANALYSIS AND GELATIN ZYMOGRAPHY

Samples were resolved by 10% SDS-PAGE and electrotransferred to a PVDF membrane (Millipore, USA). After blocking with 5% non-fat

milk in TBST for 1 h the membrane was incubated overnight at 4°C with primary Ab followed by HRP-linked secondary Ab. Proteins were visualized using ECL™ Advance Western Blotting Detection Kit (GE Healthcare, USA).

Gelatinolytic activity of MMP-2 and MMP-9 in culture supernatants was analyzed by gelatin zymography as described previously [Menshikov et al., 2006]. Conditioned medium was collected after ADSC stimulation for 18 h with TNF-α or its combination with growth factors (PDGF-BB 10 ng/ml, EGF 10 ng/ml, SDF-1α 150 ng/ml, RANTES/CCL5 150 ng/ml) in serum-free medium.

MEASUREMENT OF INTRACELLULAR REACTIVE OXYGEN SPECIES (ROS) PRODUCTION

Dihydroethidium (DHE) was used to estimate intracellular superoxide (O_2^-) production in ADSC. Confluent monolayer was scratched with pipette tip and washed. Then after 2 h, ADSC were treated with TNF-α (5 ng/ml) for 20 min, DHE was added into the medium to a final concentration of 1.25 μM and cells were incubated for 10 min. Then cells were washed with DPBS and maintained in a fresh medium during the photomicrographs acquisition at 100x magnification with Axiovert 200M fluorescent microscope (Carl Zeiss, Germany).

FIBRIN GEL BEAD ANGIOGENESIS ASSAY

Effect of ADSC pre-treatment with TNF-α on angiogenesis was analyzed using fibrin gel bead assay. Briefly, HUVEC at passage 3–4 were cultured on Cytodex microbeads (Sigma-Aldrich, USA). Beads with attached cells were labeled with 5μM CellTracker™ Green CMFDA (Life Technologies, USA) and then mixed with ADSC p 2-3 (treated with TNF-α, 5 ng/ml overnight prior to experiment or untreated) and embedded at 250 beads/well and 4×10^4 ADSC/well of a 24-well plate in a fibrin clot. After 1, 3, or 5 days of incubation, gels were fixed and imaged on confocal microscope TCS SP5 (Leica, Germany). Average sprout lengths per bead was measured using ImageJ software. Detailed description of the assay can be found in online Supplementary materials.

EXPERIMENTAL ANIMALS

We used 10–12 weeks old C57Bl6 male mice for model of hind limb ischemia. All animals received standard food and water ratios. Surgical manipulations and euthanasia protocols were designed in accordance with Institute and National regulations.

MOUSE HIND LIMB ISCHEMIA MODEL AND ADSC INJECTION

Hind limb ischemia was created by excision of femoral artery under avertin narcosis as previously described [Makarevich et al., 2012]. After surgery animals were randomly divided into three groups: the first group was administered with passage 3 mouse ADSC (8.5×10^5 cells per mouse); the second group was administered with mouse ADSC (8.5×10^5 cells per mouse) preincubated overnight with mouse TNF-α (5 ng/ml); the third group was injected with sterile saline (0.9% NaCl) used as vehicle to prepare ADSC suspensions. Cell suspensions or saline were administered by three 50 μl injections into the anterior tibial, the gastrocnemius, and the hip biceps muscles.

NON-INVASIVE EVALUATION OF HIND LIMB PERFUSION

Limb perfusion was assessed using Moor LDI 2.0 system (Moor, Great Britain) in isoflurane-narcotized animals. Blood flow interruption was controlled after surgery and subsequently perfusion dynamics was assessed at days 7 and 14 of the experiment. Laser Doppler measurement procedure is described in online Supplementary materials.

MUSCLE HARVEST AND HEMATOXYLIN-EOSIN STAINING

At day 14 mice from test groups were sacrificed by lethal isoflurane dose. After skin dissection ischemic *m. tibialis anterior* was harvested and frozen in TissueTek medium in liquid N_2. Parallel sections (7 μm) were prepared on glass slides and stored at −70° C. Routine hematoxylin-eosin staining of formalin-fixed sections was used for necrosis analysis in *m. tibialis anterior*. Stained sections were photographed using low magnification to obtain whole-section images and necrotic/infiltrated/viable tissue areas were calculated in ImageJ software. Obtained data were used for statistical analysis after being expressed as percent of section area.

MCP-1 GENE SILENCING BY shRNA

Lentiviral particles containing irrelevant or MCP1-targeted short hairpin RNA cloned along with CopGFP were purchased from Evrogen (Moscow, Russia). ADSC were transduced overnight at a MOI=10 in complete medium containing 10 μg/ml of Polybrene®. For details, see online Supplementary materials.

STATISTICAL ANALYSIS

Data are expressed as mean ± standard error of mean (s.e.m.); statistical significance of difference between values (unless other is indicated) was determined using unpaired Student *t*-test; $P<0.05$ was considered significant. Data of three serial experiments are presented unless other is indicated.

RESULTS

TNF-α STIMULATES ADSC PROLIFERATION WITHOUT SIGNIFICANT INDUCTION OF APOPTOSIS

TNF-α is a pleiotropic cytokine with diverse effects that range from triggering proliferation to inducing apoptosis, which depends on cell type, status and environment. This can be attributed to activation of two cell surface receptors—TNFRI (p55) and TNFRII (p75), which differ in signal transduction [Bradley, 2008], ligand affinity and association/dissociation kinetics [Medvedev et al., 1996]. Prior to in vitro tests, we conducted preliminary experiments using immunoblotting (see Supplementary Materials Fig. S1) and found that ADSC carry both receptors: TNFRI and TNFRII. Taking this into account we used 5 or 100 ng/ml TNF-α to stimulate cells and evaluated their viability, proliferation and apoptosis in a culture of human ADSC via several experimental approaches.

We performed MTT assay to ensure that chosen concentrations of TNF-α are non-toxic to ADSC and, moreover, TNF-α at both doses increased ADSC viability with comparable effect (Fig. 1A). As far as MTT assay relies mostly on mitochondrial activity we further analyzed TNF-α effects on proliferation by detection of Ki-67–a

nuclear marker present during active phases of cell cycle, but absent in quiescent cells (G0). We performed immunostaining of ADSC (Fig. 1C) and western blot (Supplementary Materials Fig. S1) to demonstrate that stimulation with TNF-α for 48 h increased number of Ki-67 positive cells.

To further substantiate the results of MTT-assay and Ki-67 staining we analyzed by FACS cell cycle phases distribution in ADSC labeled by propidium iodide. We found that S/G1 ratio in ADSC incubated with 5 or 100 ng/ml of TNF-α was 2.16 and 2.475 fold greater than in control cells (0.125 ± 0.012 and 0.109 ± 0.018 vs. 0.0506 ± 0.02 in control, respectively) suggesting that more cells were entering S-phase (Fig1 B). As in previous tests, we found no significant difference between two concentrations of TNF-α.

Apoptosis activation after TNF-α treatment was assayed using FITC-Annexin V and we found that TNF-α did not induce apoptosis significantly after treatment for 24 h at both concentrations. Indeed proportion of apoptotic cells was $0.45 \pm 0.05\%$; $0.33 \pm 0.03\%$ and $0.42 \pm 0.05\%$ in control, 5 and 100 ng/ml TNF-α, respectively.

TNF-α ACTIVATES ADSC CYTOSKELETON REMODELING AND MOTILITY IN VITRO

Cells ability to migrate relies much on cell cytoskeleton remodeling [Möpert et al., 2012] and required for MSCs (including ADSC) to leave the niches and penetrate through the tissue. To evaluate influence of TNF-α on rearrangement of actin cytoskeleton in ADSC we exposed them to TNF-α for 15 h. After that cells were fixed in cold methanol and filamentous actin was stained using Alexa594-labelled phalloidin in combination with anti-vinculin antibody.

Photomicrographs in Figure 2A demonstrate that control cells have less polymerized actin, mainly visible at the cell periphery in contrast to TNF-α treated cells, which developed more noticeable stress fibers and focal adhesion sites visualized by staining of vinculin. Similar data were obtained previously in experiments where fibroblasts [Puls et al., 1999] and endothelial cells [Möpert et al., 2012] were exposed to TNF-α.

Observed differences in actin filament organization may influence cell motility and contribute to cell attachment, which prompted to assay ADSC migratory response. For initial test we used a widely adopted approach—a scratch "wound" healing model. After scratching, cells were treated with TNF-α (5 or 100 ng/ml), SDF-1α, EGF, PDGF-BB or by combination of TNF-α at both concentrations with these chemoattractants. We found that TNF-α significantly promoted scratch "wound" closure alone and in combination with EGF, but not with PDGF-BB. We suggested this to occur due to strong background effect of PDGF-BB, which

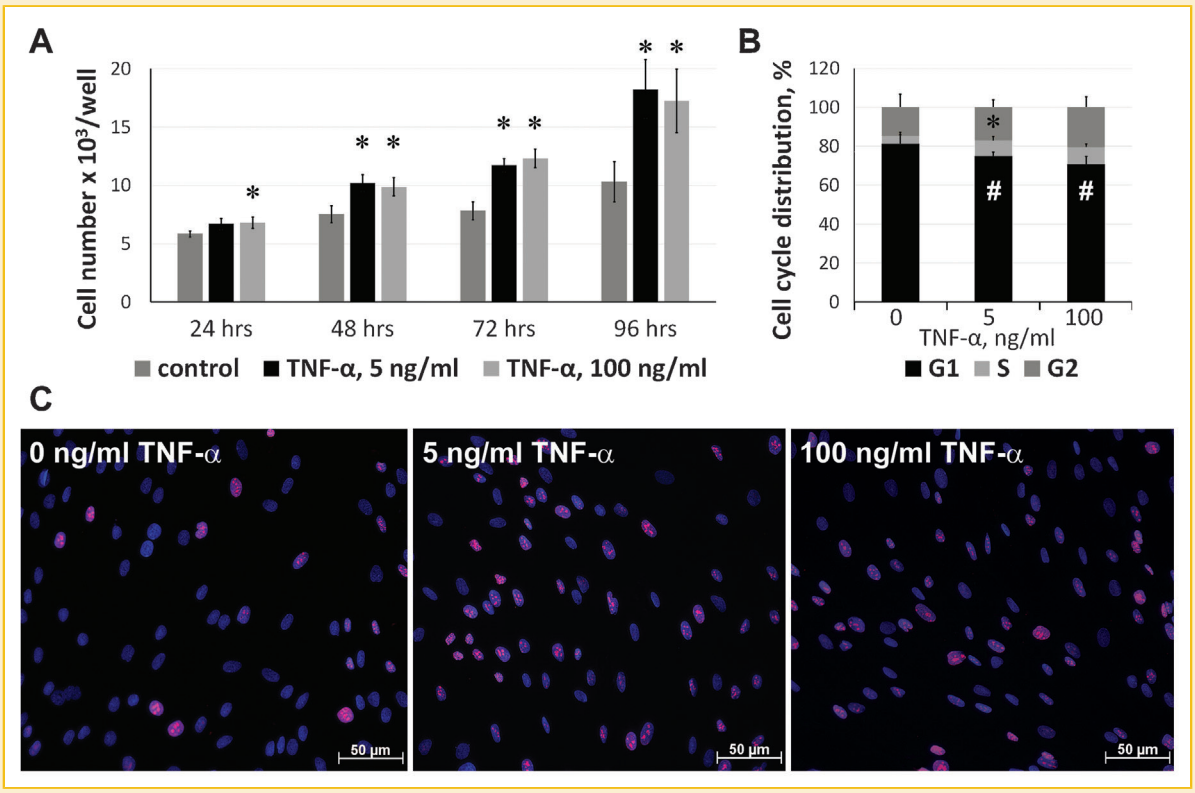

Fig. 1. Effects of TNF-α on ADSC proliferation. A. ADSC viability measured by MTT-assay. Cells were incubated in medium with 1% FBS in presence of TNF-α at 5 or 100 ng/ml. Medium was changed after 48 h of incubation. $^{*}p < 0.05$. B. FACS analysis of cell cycle distribution in ADSC labeled with propidium iodide and treated by TNF-α for 48 h. * and # denote significant ($P < 0.05$) difference in G1 and G2 cell number compared to untreated control (pair *t*-test). Mean of three independent experiments presented. C. Immunofluorescent analysis of ADSC proliferation after treatment with TNF-α at indicated concentrations for 48 h. Cells were stained using monoclonal antibodies against Ki-67 (red), nuclei stained by DAPI (blue).

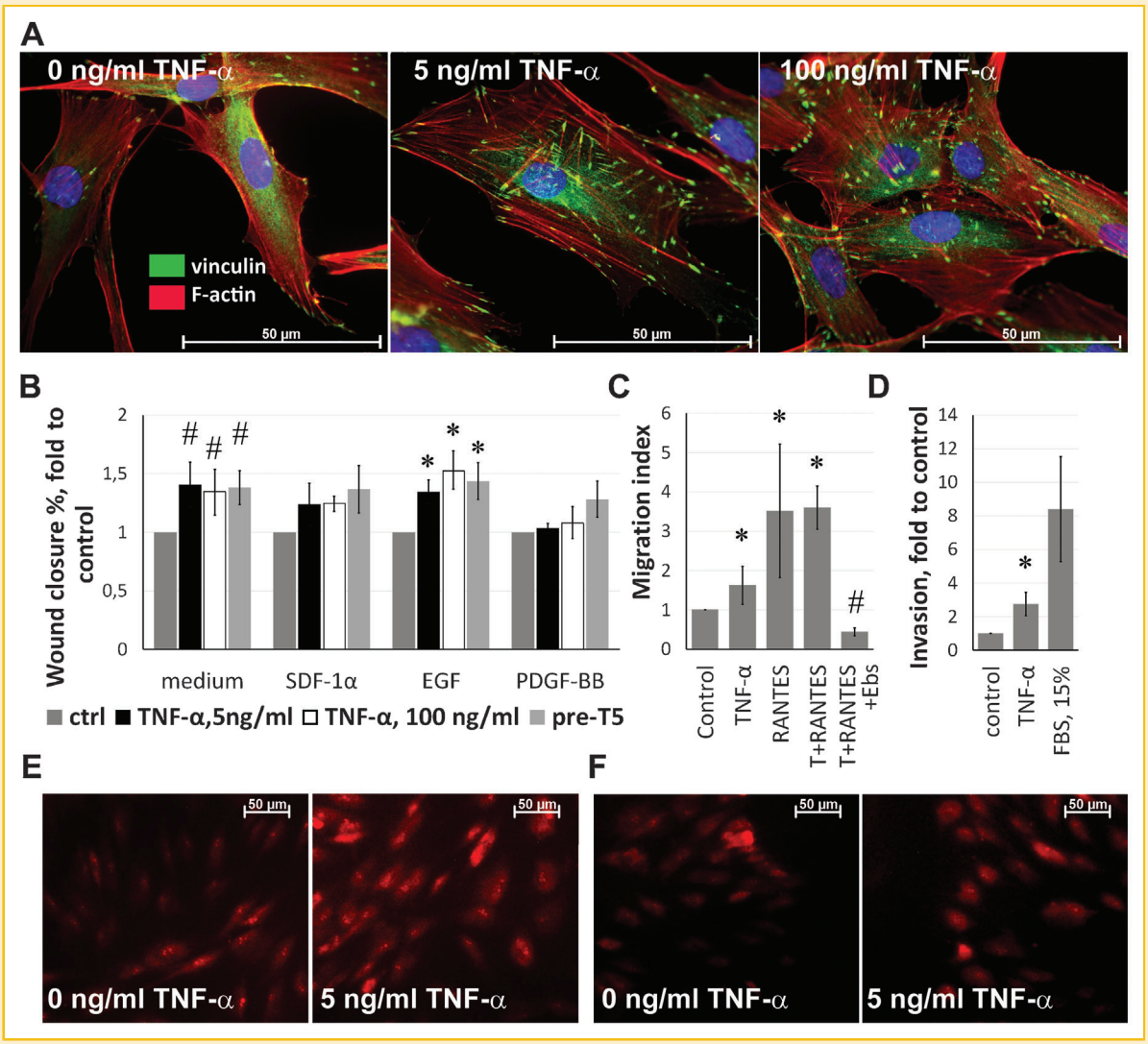

Fig. 2. TNF-α triggers actin reorganization in ADSC after 15 h of treatment by TNF-α. Focal adhesions (green) stained by anti-vinculin antibody and actin filaments stained by Alexa Fluor 594-labeled phalloidin (red). B. ADSC were grown to confluence in 6-well plates and certain wells were pre-treated with 5 ng/ml of TNF-α for 18 h before scratch "wounds" were made ("pre-T5"). Wound closure was monitored over 18 h in presence of TNF-α (0, 5 or 100 ng/ml) alone or in combination with following chemoattractants: SDF-1α (150 ng/ml), EGF (10 ng/ml), PDGF-BB (10 ng/ml). Percentage of empty area remaining 18 h after scratching was calculated and normalized to negative control (no TNF-α treatment) separately for each factor tested; $^{\#}P < 0.05$ vs. untreated cells; $^{*}P < 0.05$ vs. cells, treated with EGF alone. C. ADSC chemotaxis evaluated in a Transwell migration assay. TNF-α (5 ng/ml) and RANTES (150 ng/ml) were used as a chemoattractants; "T+RANTES"- 5 ng/ml of TNF-α was added to the upper well along with ADSC prior to migration toward RANTES; "T+RANTES+Ebs"- 5 ng/ml of TNF-α was added to ADSC, pre-treated with Ebselen (20 μM) in the upper well and cells migrated toward RANTES. Migration index was determined as number of cells that had migrated to the chemoattractants normalized to the number of cells migrated toward assay medium (DMEM, 2.5% BSA); n = 5 serial runs. $^{*}P < 0.05$ vs. control; $^{\#}P < 0.05$ vs. "T+RANTES". D. ADSC migration through Matrigel™-coated filters toward serum-free medium, 5 ng/ml TNF-α or fetal serum (15%); extent of migration toward assay medium ("Control") in each experiment was set as 1.0 and used for normalization. $^{*}P < 0.05$ for TNF-α-stimulated invasion versus control. E. Representative photomicrographs of intracellular production of ROS in ADSC visualized by DHE fluorescence after stimulation by TNF-α or saline for 20 min. F. ROS generation in wound healing assay: 2 h after scratching, ADSC were treated with TNF-α for 20 min and subsequently DHE was added into the medium.

had the highest magnitude of all cytokines (75% healed compared to 48% in EGF and 29% in SDF-1α) making it difficult to indicate TNF-α effects (Fig. 2B). Since scratch wound healing is a coordinated process involving cell proliferation and migration, we assessed influence of TNF-α on ADSC migration specifically in Transwell. We conducted this assay in two variants: using filters coated with type I collagen or Matrigel™ to assess cell migration through the tissue matrix.

In collagen-coated Transwell we found ADSC migration to be potentiated by 5 ng/ml TNF-α approximately 1.5-fold when it was added to the lower chamber. Still ADSC migration toward RANTES did not increase when TNF-α was added to the upper compartment of Transwell system (Fig. 2C). Previously it was reported that at 100 ng/ml TNF-α induces ADSC migration 6.6-fold and that prestimulation with 100 ng/ml TNF-α for 24 h can enhance migration toward RANTES by about twofold [Baek et al., 2011].

ADSC migration through Matrigel™ (modeling invasion process) was also enhanced by TNF-α ~2.5-fold (Fig. 2D) compared to assay medium ("control"), which was consistent with previous report in bone marrow MSC [Böcker et al., 2008].

TNF-α-INDUCED INCREASE IN ADSC MOTILITY CORRELATES WITH REACTIVE OXYGEN SPECIES GENERATION

To identify the role of reactive oxygen species (ROS) in TNF-α-induced cell migration we used ebselen—an antioxidant inhibitor of ROS genereation (Azad et al., 2014). Ebselen significantly inhibited ADSC migration triggered by TNF-α and RANTES (Fig. 2C) suggesting that redox component has impact on ADSC motility. Using ROS-sensitive compound—dihydroethidium (DHE) we observed significant increase in DHE fluorescence after ADSC exposure to TNF-α suggesting an escalated superoxide production (Fig. 2E).

To further substantiate our data we conducted scratch "wound" healing experiments in ADSC labeled with DHE. We found that cells located in proximity to the scratched edge, which are known to be most actively migrating, had the highest increase of DHE fluorescence (Fig. 2F). Similar increase of ROS quantity in scratched edge area was previously observed in HUVEC [Ikeda et al., 2005].

TNF-α ENHANCES ADSC INTERACTION WITH MONOCYTES AND ENDOTHELIAL CELLS

Inflammatory microenvironment probably influences ADSC potency to interact with immune and vascular cells. This may rely on paracrine modulation of ADSC function via inflammatory cytokines including TNF-α and therefore we analyzed its influence on interaction of ADSC with monocytes or endothelial cells.

First we performed adhesion assay under static conditions in which suspended THP-1 monocytes were seeded on top of ADSC monolayer. In these experiments, pretreatment of ADSC with TNF-α significantly potentiated monocyte adhesion to them (Fig. 3A). Moreover, additional increase of THP-1 adhesion was observed when ADSC's conditioned medium was not aspirated prior to monocytes addition (Fig. 3A). In that case monocytes and ADSC interacted in presence of factors, produced by the latter during 18 h pre-incubation with TNF-α, which had a potentiating effect.

Next we evaluated whether pre-treatment of ADSC with TNF-α for 18 h could influence their adherence to endothelium (HUVEC). We found that ADSC pre-treated with TNF-α had lower adherence to HUVEC, but this effect was observed only at an early time point (40 min) representing initial cell-to-cell interaction. At a later stage when cell spreading occurs (approximately 120 min) pre-treatment with TNF-α had no significant influence on ADSC and HUVEC interaction (Fig. 3B).

We also performed a triple adhesion experiment where mixed suspension of green-labeled ADSC and red-labeled THP-1 was seeded on top of unstained HUVEC monolayer. Fluorescent staining allowed us to distinguish between ADSC and monocyte adhesion to endothelium after incubation and we found that pre-treatment of ADSC with TNF-α decreased amount of ADSC adherent to HUVEC compared to untreated control. Interestingly number of adherent THP-1 was also decreased in TNF-α pretreated ADSC specimen (Fig. 3C), which suggests that ADSC/monocyte complexes were formed and washed away resulting in concordant decline of both cell types' adhesion to HUVEC.

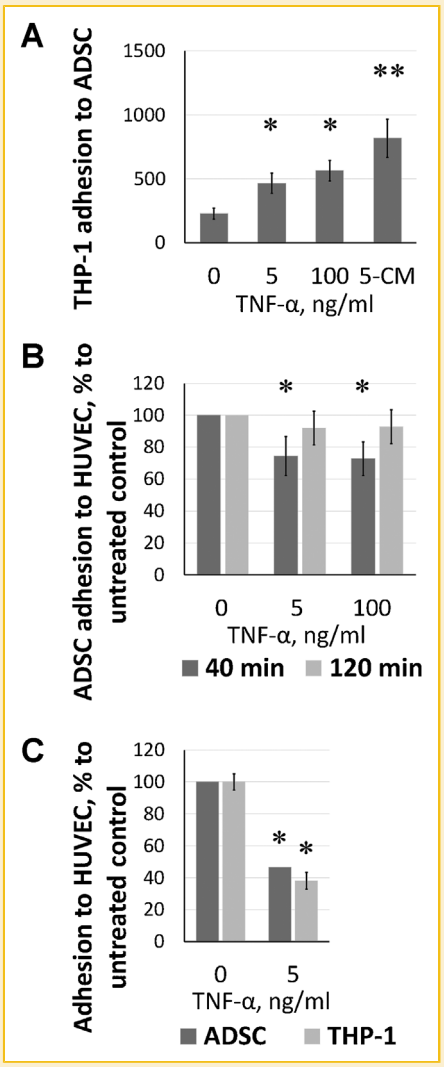

Fig. 3. TNF-α modulates interaction between ADSC and monocytes or endothelial cells. A. Adhesion of THP-1 to ADSC monolayer was evaluated in a static adhesion assay. ADSC were preincubated with TNF-α at indicated concentrations overnight and conditioned medium was replaced by fresh except in specimen illustrated in last column ("5-CM"). THP-1 cells were seeded over ADSC monolayer for 40 min, unattached cells were washed and adherent cells were counted in microscope images in at least 5 FOV; B. ADSC pretreated with TNF-α or saline for 18 h were stained by CellTracker™ Green CMFDA and seeded on top of HUVEC monolayer. After 40 or 120 min unattached cells were washed. Remaining cells were photographed and attached cell counts were normalized by number of adherent cells in control set as 100%; C. Labeled ADSC pretreated overnight with TNF-α or saline were mixed with labeled THP-1 monocytes and seeded over unstained HUVEC monolayer and after 40 min unbound cells were washed. Number of adherent ADSC and THP-1 in control samples was set to 100% and used to normalize the data obtained from TNF-α-stimulated ADSC; $^{*}P < 0.05$ compared to control cells ("0 ng/ml").

TNF-α INCREASES ADSC PROTEOLYTIC POTENTIAL VIA PRODUCTION OF MMP-9 AND ACTIVATION OF MMP-2

To migrate through ECM cells employ local proteolysis by matrix metalloproteases (MMPs) and plasminogen activators (i.e., uPA). In our model we observed enhancement of ADSC migration through Matrigel™ toward TNF-α (5 ng/ml) (Fig. 2D). To determine whether TNF-α can induce MMPs expression in ADSC as it does in a variety of cell types [Moon et al., 2004] gelatin substrate zymography was performed. After we found (Fig. 4A) that treatment of ADSC by TNF-α increased level of MMP-9, but not of MMP-2 in culture medium, MMP-9 and MMP-2 activity was quantified by densitometry using ImageJ software (Fig. S1C). Data analysis showed that MMP-2 proteolytic activation occurred during incubation with TNF-α, which suggests that despite total amount of MMP-2 was stable proportion of activated MMP-2 (proteolytically active MMP-2 with lower molecular weight) was higher after TNF-α treatment. Notably no other tested chemoattractant (PDGF-BB, EGF, SDF-1α, or RANTES) altered TNF-α effects or induced MMP-2/MMP-9 production or their activation. These results were supported by data obtained in real-time PCR (see Table II), which indicated that treatment of ADSC with TNF-α for 18 h at 5 or 100 ng/ml strongly increased MMP-9 and uPA mRNA level as well as no significant increment of MMP-2 expression was found.

TREATMENT OF ADSC BY TNF-α INDUCES EXPRESSION OF ANGIOGENIC PROTEINS, INFLAMMATORY CYTOKINES AND ICAM-1

Assuming that ADSC could contribute to angiogenesis via paracrine activity we used RT-PCR to study whether TNF-α modulates expression of proangiogenic factors genes. Data presented in Table II indicates that TNF-α moderately up-regulates ANGPT-1, FGF2, and VEGF mRNA levels, but strongly increases expression of MCP-1. As for interleukin-8 (IL-8) we found a dramatic increase of its mRNA and protein levels induced by TNF-α (Fig. 4D).

Stimulation with TNF-α also resulted in significantly increased expression of pro-inflammatory factors mRNA including IL-1β and IL-6 (Table II). As for anti-inflammatory factors like TGF-β or

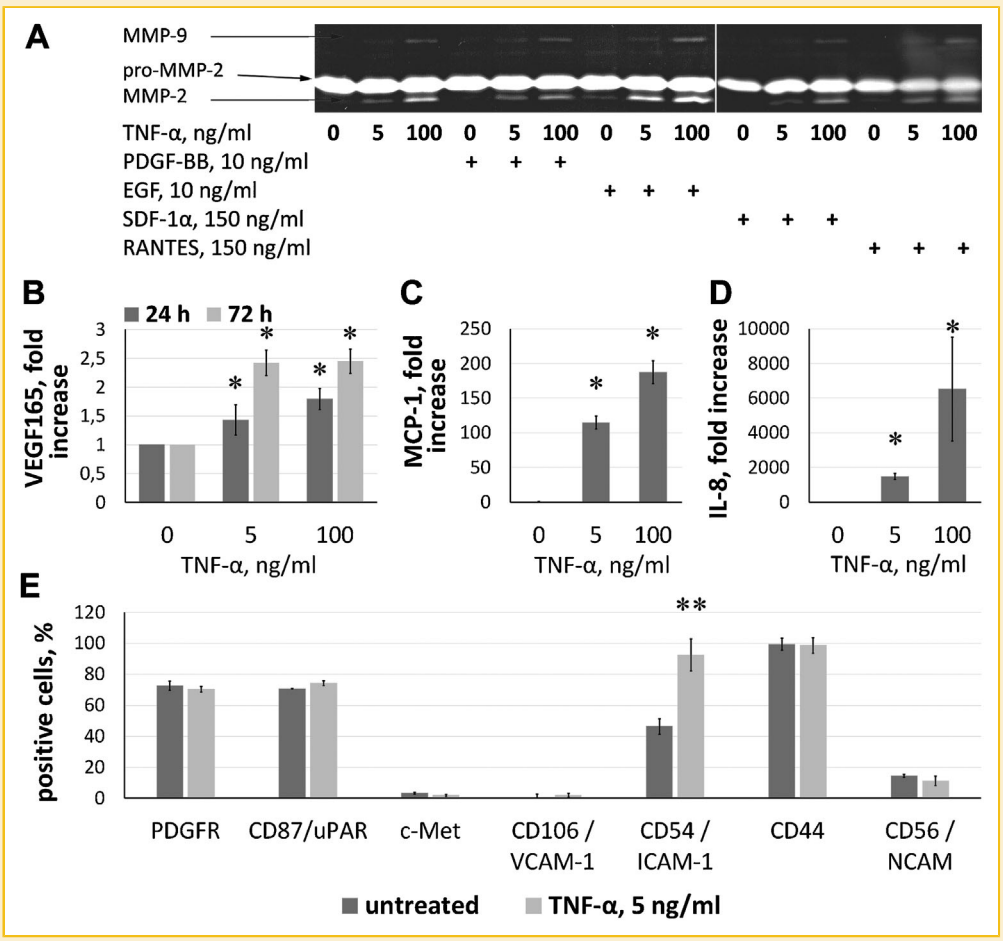

Fig. 4. ADSC stimulation by TNF-α induces expression of proangiogenic, inflammatory and migration associated proteins. A. Secretion and activation of MMP-2 and MMP-9 were evaluated after ADSC pretreatment by TNF-α alone or in combination with either SDF-1α (150 ng/ml), EGF (10 ng/ml), PDGF-BB (10 ng/ml), or RANTES (150 ng/ml). Initially ADSC were incubated for 1 h in serum-free medium with PDGF-BB, EGF, SDF-1α or RANTES and then TNF-α was added to the cells. After overnight incubation, conditioned medium was collected and analyzed by substrate zymography. B. Concentration of VEGF165, MCP-1 and IL-8 was measured in ADSC culture medium by ELISA after treatment of ADSC with TNF-α for 24 or 48 h. C. FACS analysis of PDGFR, uPAR, c-Met, VCAM-1, ICAM-1, CD44 and NCAM cell surface expression after treatment with 5 ng/ml of TNF-α overnight; $^{*}P < 0.05$ or $^{**}P < 0.01$ compared to untreated ADSC.

TABLE II. List of Significant Changes of mRNA Expression in ADSC After Stimulation With TNF-α

	TNF-α concentration			TNF-α concentration	
Gene	5 ng/ml	100 ng/ml	Gene	5 ng/ml	100 ng/ml
ANGPT1	2.7 ± 1.6	1.6 ± 0.9	MMP-9	15.1 ± 3.9	11.5 ± 4.2
FGF-2	2.8 ± 2	2.4 ± 1.1	MCP-1	103.6 ± 56	109.5 ± 49.1
ICAM-1	22.4 ± 0.5	16.1 ± 0.3	PAI-1	2.9 ± 1	3.1 ± 2
Il-1β	39.7 ± 20.8	42 ± 34	*PPAR-γ*	*0.5 ± 0.3*	*0.4 ±0.1*
Il-4	*0.6 ± 0.2*	*0.4 ± 0.1*	*TGF-β*	*0.7 ± 0.1*	*0.6 ± 0.1*
Il-6	14.3 ± 5.3	14.1 ± 6.4	uPA	1.9 ± 0.6	1.3 ± 0.1
Il-8	1864.9 ± 324.6	3071.3 ± 937.7	uPAR	1.4 ± 0.3	1.5 ± 0.2
Leptin	*0.8 ± 0.2*	*0.7 ± 0.2*	VCAM-1	11.9 ± 4.3	10.4 ± 0.7
MMP-1	1.2 ± 0.1	1.1 ± 0.4	VEGF	2.1 ± 0.7	1.8 ± 0.4

Bold font indicates fold mRNA expression increase, *italic font* indicates fold decrease.
All listed changes of genes expression means (N=7 serial runs) were statistically significant ($P < 0.05$).

PPAR-γ (anti-inflammatory and proadipogenic) stimulation by TNF-α did not modulate their expression, as well as that of leptin and IL-4. Results obtained by PCR were verified using ELISA and we found that conditioned medium from ADSC treated by TNF-α had significantly higher concentrations of VEGF165, MCP-1 and IL-8 compared to untreated cells (Fig. 4B–D).

ADSC express several adhesion molecules known to act as homing receptors for hematopoetic cells. The list includes VCAM-1, ICAM-1, hyaluronic acid receptor CD44, c-met, and NCAM/CD56 - an adhesion receptor involved in cancer cell invasion [Shi et al., 2012]. Using FACS and RT-PCR we analyzed influence of TNF-α (5 ng/ml, 24 h) on expression of these adhesion factors in ADSC. Our data (Fig. 4E) show that TNF-α markedly increased expression of ICAM-1, but not VCAM-1. The latter was found in barely detectable amounts in untreated ADSC and after incubation with TNF-α showed minimal expression increase within detection limits. Expression of c-met, CD56, and CD44 was not influenced by TNF-α.

EFFECTS OF TNF-α ON MAPK, Akt AND Rac1 ACTIVATION IN ADSC

Observed effects of TNF-α on a variety of ADSC functions suggested involvement of specific downstream effector molecules. Among them MAP-kinases and Akt are the key signaling regulators of numerous cellular functions including angiogenesis, cell metabolism, proliferation, motility, and survival.

We found that level of phosphorylated p-Akt was increased as early as after 15 min of exposure of ADSC to TNF-α at 5 ng/ml (Fig. 5A) and was persistent after overnight incubation with TNF-α (Fig. 5B). Kwon et al. [2000] reported that Akt can directly phosphorylate Rac1 at Ser71; in addition in pull-down assay it was shown that phosphorylated Rac1 is in its active conformation [Schoentaube et al., 2009]. Therefore we studied Rac1 phosphorylation after ADSC treatment with TNF-α and found pRac-1 (S71) level to be increased after 30 min of incubation with TNF-α (Fig. 5A) suggesting modulation of Rac1 activity by this cytokine.

It has been reported that both Rac1 and Akt are involved in activation of NF-κB [Ozes et al., 1999; Schwarz et al, 2012]. NF-κB activation is primarily regulated by phosphorylation and subsequent proteasome degradation of an inhibitory subunit—IκB. In our experiment level of IκB decreased at 15 min of ADSC exposure to TNF-α, which corresponds to rapid NF-κB activation (Fig. 5A). It was shown by Böcker et al. that NF-κB activation is essential for basal or TNF-α-induced proliferation of bone marrow MSC.

In addition we found that TNF-α induces phosphorylation of ERK1/2 and p38 MAP kinases (Fig. 5A), which mediate proliferative and pro-invasive effects in a number of cell types, including ADSC [Boutros et al., 2008]. Quantitative densitometry and statistical analysis of the Western blotting data are shown in Supplementary materials Fig. S2.

To evaluate a possible role of ROS and Akt in ADSC proliferation we conducted MTT assay with two compounds—TIRON and LY294002, which are cell permeable ROS scavenger and PI3K/Akt inhibitor respectively. Treatment by TIRON resulted in decline of TNF-α-induced ADSC proliferation (Fig. 5C), yet TIRON itself showed no significant influence on untreated cell number (data not shown). Furthermore, by the end of assay (96 h) we found that in TNF-α-treated ADSC addition of TIRON reduced cell count compared to control treated by TIRON alone. We also found that addition of LY294002 resulted in a decline of Akt phosphorylation (data not shown) and reduction of TNF-α prosurvival effect at 24 h time point (Fig. 5C).

TNF-α POTENTIATES ADSC PROANGIOGENIC ACTIVITY IN A FIBRIN GEL BEAD MODEL

ADSC support and potentiate endothelial vessel formation in model of angiogenesis in fibrin gel [Rohringer et al., 2014]. To examine whether TNF-α can enhance ADSC ability to stabilize and promote growth of microvessels HUVEC-coated beads were co-cultured with ADSC pre-treated with 5 ng/ml of TNF-α and uniformly distributed throughout fibrin gel. Cultures were maintained for 1, 3, and 5 days and z-stack images were taken using confocal microscope. We observed that at day 1 sprouts were barely visible (see Supplementary Materials Fig. S2), but at day 3 HUVEC co-cultured with TNF-α-treated ADSC demonstrated significant increase in both—microvessel length and density comparison to co-cultures with untreated ADSC (Fig. 6A). Quantification of images also revealed that presence of TNF-α-pretreated ADSC significantly stimulated microvessel elongation and branching at 3 day, but this effect became less prominent by day 5 (Fig 6B). High-magnification images of the individual beads provided in Supplementary Materials Fig. S2.

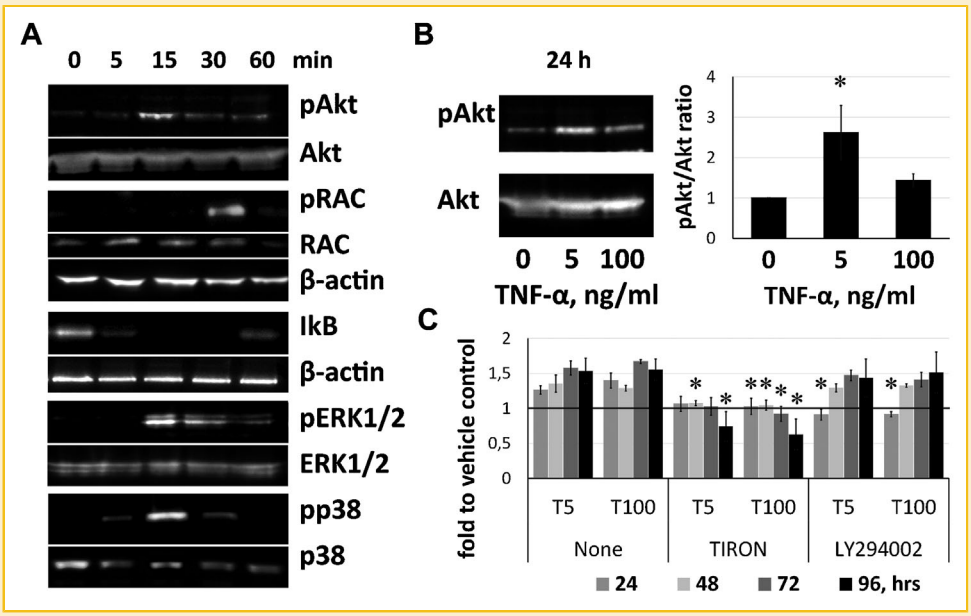

Fig. 5. Intracellular signal transduction induced in ADSC by TNF-α. A. Phosphorylation of Akt, Rac1, ERK, p38 and IκB degradation after ADSC treatment with TNF-α (5 ng/ml) was evaluated by Western blot analysis. To normalize for protein loading, all membranes were reprobed with anti-Akt, Rac1, ERK, p38 and β-actin antibodies; B. Akt phosphorylation was assayed after cell stimulation with TNF-α for 24 h; photographs were quantified by densitometry in ImageJ software; data presented as p-Akt to Akt ratio; $^{*}P < 0.05$ compared to untreated control; C. Effect of signal transduction inhibitors on TNF-α effects evaluated by MTT assay. ADSC were treated with TNF-α (5 or 100 ng/ml) along with the following inhibitors: ROS scavenger Tiron (3 mM) and PI3-K inhibitor LY294002 (1 μM). Assay medium was replaced by fresh at 48 h of incubation. Data were acquired after 24, 48, 72, or 96 h and expressed as fold change to untreated control for each inhibitor separately. $^{*}P < 0.05$ versus "T5" and "T100".

To examine lumen formation and ADSC-HUVEC interaction at a higher resolution ADSC were labeled with PKH26 and images of single vessels were taken indicating that by day 5 most of the sprouts formed a visible lumen. Moreover, ADSC seemed to align closely to the sprouts acting in a pericyte-like manner (Fig. 6C and Supplementary materials Fig. S2), which may putatively indicate their participation in blood vessel stabilization.

INHIBITION OF MCP-1 COMPROMISES ENDOTHELIAL CELL SPROUTING IN A CO-CULTURE WITH TNF-α-PRE-TREATED ADSC IN A FIBRIN GEL

Our data indicate that treatment by TNF-α increases MCP-1 expression by ADSC more than 100-fold (Fig. 4). MCP-1 is known to have direct effect on promoting angiogenesis in rat aortic ring sprouting assay [Salcedo et al., 2000] and plays a cornerstone role in arteriogenesis stimulation in ischemic tissue [van Amerongen et al., 2007]. We speculated that stimulation of angiogenic response by TNF-α–treated ADSC may be mediated by increased production of this chemokine. To evaluate this hypothesis we used lentivirus mediated RNA interference to silence MCP-1 expression in ADSC. Efficiency of transduction was estimated by fluorescent microscopy and had a value of approximately 70% in P 2-3 ADSC (Supplementary materials Fig. S3). MCP-1 silencing efficiency assessed by ELISA of culture medium showed drastic decline (~73%) of chemokine concentration after delivery of shRNA-MCP-1 compared to ADSC infected with irrelevant shRNA and uninfected ADSC (2006.16 ± 341 pg/ml vs. 5603.78 ± 167 pg/ml vs. 10367.8 ± 1678 pg/ml, respectively).

In a fibrin gel bead angiogenesis assay uninfected or MCP-1-silienced ADSC were pretreated with 5 ng/ml of TNF-α overnight and then co-cultured for 3 days with HUVEC-coated beads. We found that silencing of MCP-1 in ADSC resulted in significant reduction of mean sprouts length per bead: 166 ± 47 μm versus 226 ± 51 μm in ADSC infected with shRNA-ctrl, $P < 0.001$ (Supplementary materials, Fig. S4B) and there was a non-significant trend toward fewer sprouts number per bead (8.89 ± 3 vs. 10.43 ± 4, $P = 0.09$).

To support our data we also used an Ingramon—a synthetic peptide fragment (65–76) of MCP-1, which interferes with MCP-1 binding to heparin and blocks its cellular effects [Arefieva et al., 2011]. Addition of Ingramon to the assay medium reduced average length of endothelial sprouts per bead (121.5 ± 38 μm vs. 152.17 ± 54 μm in control; $P < 0.001$) but had no inhibitory effect on tubes number per bead (5.3 ± 3 vs. 4.7 ± 3; $P = 0.27$) (see Supplementary Materials Fig. S4C).

BLOOD FLOW RECOVERY IN MOUSE HIND LIMB ISCHEMIA MODEL INDUCED BY ADSC PRETREATED WITH TNF-α

After surgical induction of limb ischemia (day 0) perfusion in most animals dropped to 5–7% compared to non-operated limb (Fig. 7B). Subsequent blood flow recovery was evaluated at day 7 and 14 by laser Doppler measurement. Dynamics of perfusion in ischemic limbs after injection of saline (0.9% NaCl), control cells ("ADSC") or cells pretreated with TNF-α ("ADSC+TNF-α") has shown significant difference between experimental groups at day 7 with maximal blood flow recovery in ADSC+TNF-α animals (perfusion increase up

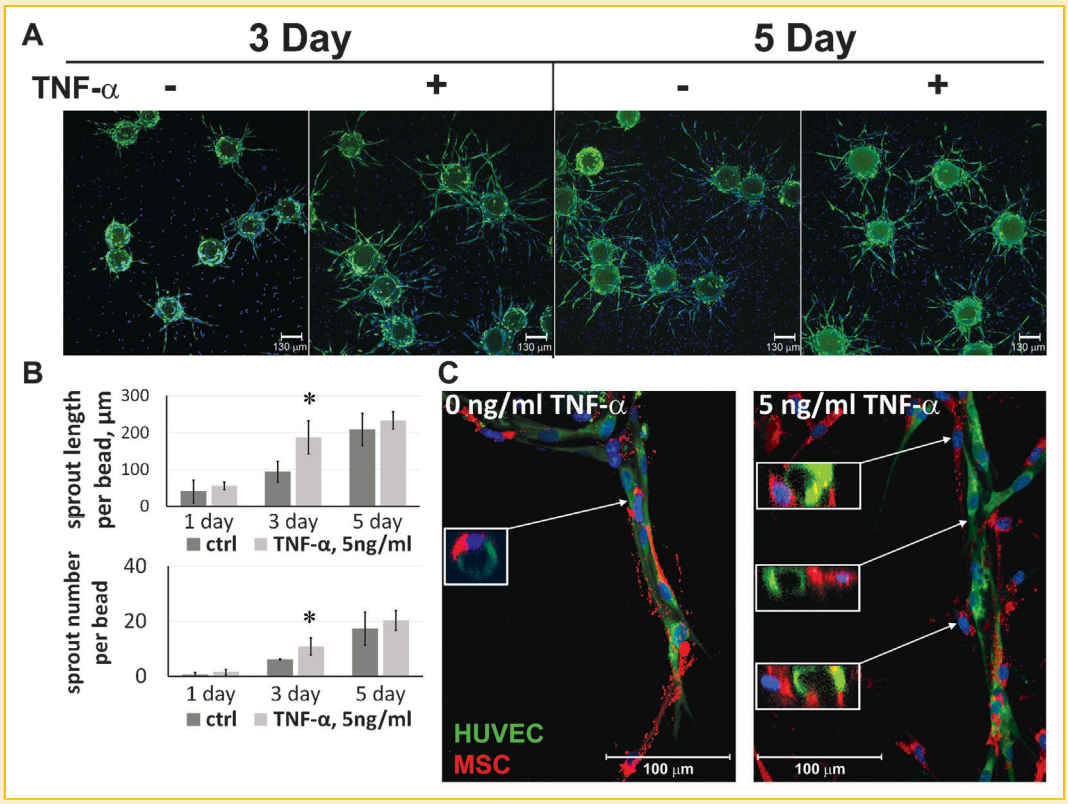

Fig.6. ADSC pretreatment with TNF-α facilitates microvessel formation in 3D ADSC/HUVEC co-culture. A. Representative images of fibrin gel bead angiogenesis assay obtained at days 3 and 5 of co-culture. HUVEC (green) were cultured on microcarrier beads and suspended in a fibrin gel with ADSC (not labeled) pretreated with 5 ng/ml of TNF-α or under normal conditions for 18 h. Nuclei were stained with DAPI; B. Quantification of HUVEC sprouting in fibrin gel bead angiogenesis assay in presence of untreated ADSC or ADSC preincubated with TNF-α for 18 h. Data expressed as mean sprout length per bead and number of sprouts/bead; $^{*}P < 0.05$ vs. untreated ADSC. C. Confocal images acquired at high-power magnification show vascular tubes with a lumen formed by HUVEC (green) after 5 days of co-culture in presence of ADSC (red). Cell nuclei are stained with DAPI. Each boxed region shows x–z cross-section cutting through the endothelial sprout that contains ADSC alongside with endothelial cells forming a tubular structure with a visible lumen.

to 31.6 ± 9%). At Day 14 difference perfusion curves were nearly aligned and differences between groups were non-significant.

PRETREATMENT OF ADSC WITH TNF-α MITIGATES MUSCLE NECROSIS AND INCREASES TISSUE INFILTRATION BY INFLAMMATORY CELLS

Muscle necrosis assessment is an important endpoint reflecting tissue protection and/or induction of muscle regeneration. As far as rodents rarely develop typical ulcerative lesions we applied a morphometry test previously established by our group [Shevchenko et al., 2013]. In hematoxylin-eosin stained sections of muscle extracted from test animals at study endpoint we found administration of ADSC to result in significant decrease of necrotic fibers area. The latter were defined as anucleic myofibers with disrupted morphology and strong eosin retain in staining (Fig. 7B, D). Moreover in ADSC group necrosis span decrement resulted in higher viable fibers area with moderate yet significant drop of inflammatory infiltration (Fig. 7D).

In samples from ADSC+TNF-α group we found that span of necrotic tissue was even lower than in ADSC group and was also significantly decreased vs. negative control vehicle-treated animals. Area of viable fibers in this group was expectedly higher that in negative control and did not show any significant difference vs. untreated ADSC. Interestingly we found that pretreatment of ADSC with TNF-α led to a significant increase of inflammatory invasion to ischemic muscle. Sections from ADSC+TNF-α animals had higher area of cellular infiltrate compared to ADSC group and this indicator reached the value close to negative control vehicle-treated specimen (Fig. 7D).

ADSC PRETREATED WITH TNF-α INDUCE ARTERIOGENESIS IN ISCHEMIC SKELETAL MUSCLE

Response of ischemic tissue to restore its perfusion relies on several reactions of which angio- and arteriogenesis are of crucial importance. Gross assessment of limb perfusion by laser-Doppler is often accompanied by blood vessel density in tissue sections and we applied conventional vessel counts to evaluate capillary (CD31+ dot-like vessels) and arteriole (α-SMA+ vessels with lumen) (Fig. S5).

Our data indicate that administration of both—untreated ADSC and ADSC pretreated by TNF-α—resulted in significant increment of capillary density by day 14 of the study. Still, there was a tendency to higher amount of capillaries in ADSC group versus ADSC+TNF-α

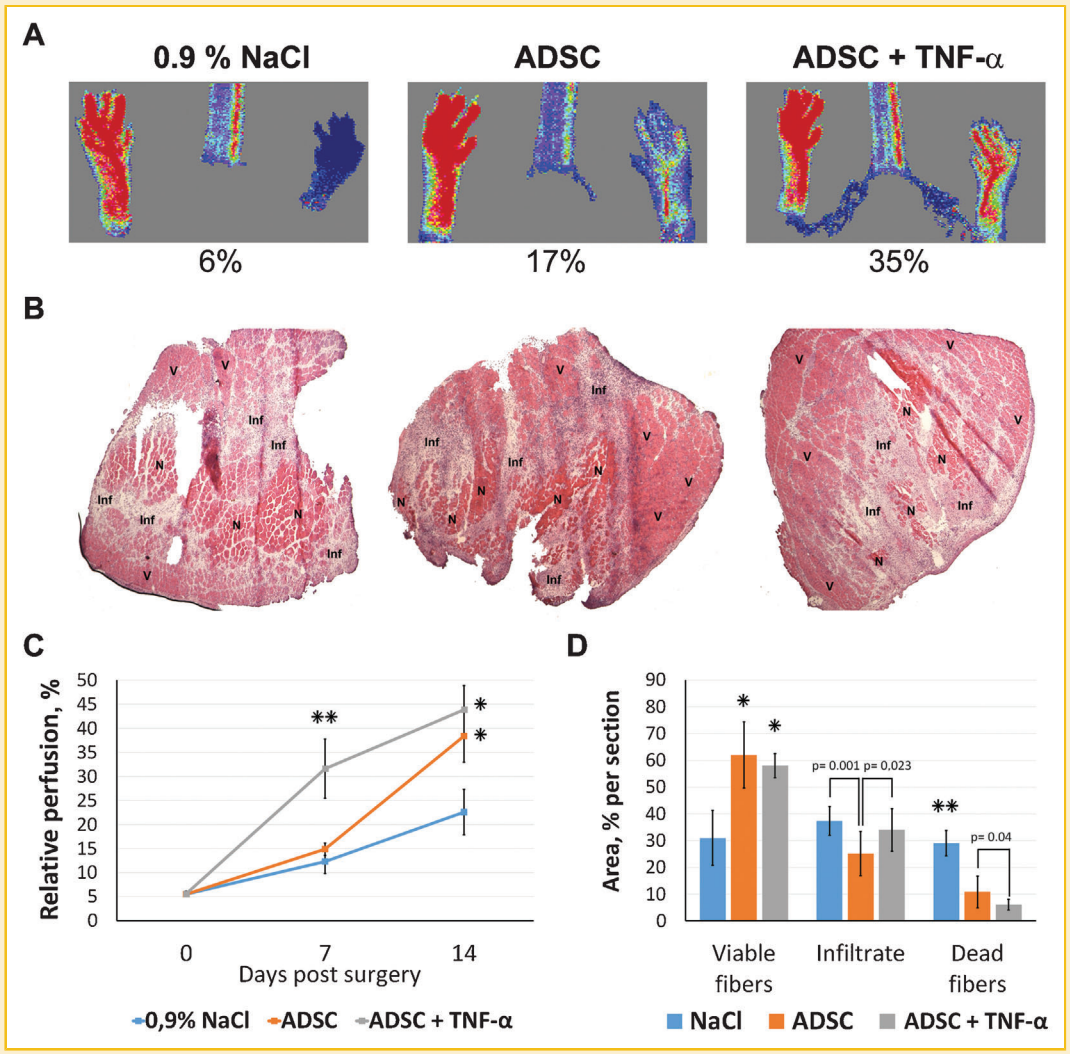

Fig. 7. Perfusion improvement and necrosis reduction in mouse ischemic hind limb after ADSC administration A. Representative laser Doppler scans of subcutaneous blood flow in mice from "NaCl", "ADSC" and "ADSC+TNF-α" groups at the day 7 after surgical ischemia induction and cell administration. B. Reduction of necrotic tissue in "ADSC+TNF-α" group is accompanied by increased infiltration of skeletal muscle. After sacrifice of animals from test groups at Day 14 m. tibialis anterior specimen were harvested, stained by hematoxylin-eosin and analyzed using whole-section images in ImageJ. V, viable skeletal muscle (including "young" fibers with centrally located nuclei); Inf, infiltrated tissue (inflammatory cells and resorbed cell debris); N, necrotic tissue (characterized by aseptic necrosis signs: loss of nuclei, disrupted fiber morphology). C. Blood flow recovery (Mean±s.e.m.) at different time points after intramuscular injection of saline (0.9% NaCl), ADSC or ADSC pretreated by TNF-α; * $P<0.005$ vs. 0.9% NaCl, ** $P<0.05$ vs. ADSC group. D. Quantitative analysis of viable/infiltrated/necrotic tissue in skeletal muscle sections was performed by morphometry. Data are expressed as % of section area (Mean±s.d); ANOVA and Student's *t*-test with Bonferroni correction was applied for statistical analysis of data; $^{*}P<0.001$ vs. NaCl group; $^{**}P<0.001$ versus ADSC and ADSC+TNF-a group.

and it reached statistical significance ($P=0.01$). As for large caliber α-SMA+ vessels (approximately 30–100 μm) we found that only in specimen from ADSC+TNF-α group density of these vascular structures was increased compared to negative control group (Table III). Thus, it is likely that pre-treatment of ADSC with TNF-α alters their pro-angiogenic capacity switching it toward arteriogenic response which was robust only in animals from this group.

DISCUSSION

Regeneration requires a finely tuned interplay between angiogenesis and inflammation triggered by homeostasis disturbance due to infection, toxins, ischemia or other kind of stress. Inflammation is the initial potent reaction, which generates new environment filled with inflammatory cells and cytokines released by them and other cell types. All these changes create conditions for further regeneration and accompanying vessel growth.

Involvement of MSCs in tissue repair is well-known, and their role is not limited to paracrine secretion of growth factors and cytokines. MSCs can differentiate and replace damaged or necrotic tissue elements, participate in circulating progenitor cells homing and modulate a wide spectrum of reactions including vessel growth and inflammation itself. These properties put MSCs in a pivotal position for postnatal tissue regeneration. Thus, interplay between them and inflammatory environment become a crucial

TABLE III. Results of Histological Vascular Density Analysis in Skeletal Muscle of Animals From Experiments Groups

Test Group	CD31+ vessels	*P*-value	α-SMA+ vessels	*P*-value
NaCl	191.2 ± 11.9	–	2.1 ± 0.3	–
ADSC	252.8 ± 18.3	0.001*	2.2 ± 0.2	0.416*
ADSC+TNF-α	225.8 ± 10.0	0.01**	3.1 ± 0.3	0.03**

Data presented as M ± SEM (Mann–Whitney U-test)
*P versus NaCl group.
**P versus ADSC group.

aspect for understanding of their mode of action and regenerative potential.

Paracrine stimuli seems to be the key factors that "prime" MSC and drive them out of their niches to facilitate regeneration. One of major cytokines in acute inflammation is TNF-α, which is known to have receptors on virtually every cell type and to evoke multiple biological responses from stimulation of cell growth and differentiation to triggering apoptosis.

Diversity of TNF-α effects is may in part be explained by existence of two receptors, which differ in ligand affinity [Medvedev et al., 1996] and have a cross-talk between their signaling pathways despite being activated independently thus, maintaining a delicate balance between cell survival and apoptosis [Naudé et al., 2011]. It was reported that in wound healing assay TNF-α induces migration of epithelial cells at 1 ng/ml via TNFRII, but completely blocks their migration at 100 ng/ml by activation of TNFRI [Corredor et al., 2003]. We found that ADSC carry both receptors (Fig. S1A) and, thus, can be prone to both – "positive" and "negative" effects of TNF-α. As far as in vitro models depend on cytokine quantity we used two concentrations of TNF-α – 5 or 100 ng/ml and found both of them to enhance ADSC proliferation, migration and expression of angiogenic factors. Notably, we did not observe any apoptotic or toxic effects of TNF-α on ADSC at both concentrations. However, we decided to apply pretreatment at a lower concentration of TNF-α when studying growth of microvessels and in our animal test to reduce chance of TNF-α toxicity.

In our experiments we used a number of supporting methods (MTT assay, Ki-67 staining, cell cycle analysis) and found that TNF-α induces ADSC proliferation (Fig. 1 A–C). This can be beneficial for tissue repair and angiogenesis due to increased number of elements capable to substitute injured cells and secrete trophic factors. In addition, we demonstrated that TNF-α-induced increase in ADSC proliferation may be mediated by ROS production and activation of PI3K pathways: addition of ROS scavenger or PI3K-specific inhibitor reduced cell survival and number of cells at experiment endpoint after TNF-α treatment (Fig. 5C).

Another important observation concerned ADSC's actin cytoskeleton rearrangement and enhanced motility after treatment with TNF-α (Fig. 2). These changes may contribute to migration of ADSC to the site of injury and their recruitment from the niche. Indeed, in "wound closure" assay we showed that TNF-α-treated ADSC had higher migratory potential. Suggested role of ROS in enhancement of cell motility was supported by experiments with DHE, which detected intensive generation of ROS on the margin of the "wound". Influence of ROS-scavenger (ebselen) on TNF-α-induced ADSC motility also indicated importance of redox component in observed changes (Fig. 2C, E, and F).

MSC movement through tissues also requires certain "way-making" abilities and proteolytic potential mediated by MMPs, uPA and other proteins that cleave ECM. Up-regulation of uPA and MMP-9 expression was detected by RT PCR and verified by zymography. Notably MMP-2 expression remained at baseline in PCR tests, which correlated with zymography results that detected no change in full-length MMP-2 level. However, we found increased amount of cleaved MMP-2 prompting activation after TNF-α treatment rather than its de novo production.

As for adhesion and homing-related molecules assayed in PCR and FACS we found only ICAM-1 to be significantly up-regulated in stimulated ADSC. ICAM-1 is crucial for cell-to-cell interaction and adhesion [Long, 2011] and our data suggested assessment of ADSC adhesive properties after TNF-α stimulation.

In attempt to simulate cell interaction in angiogenesis under inflammatory conditions we studied influence of TNF-α on adhesive properties in three cell types: monocytes, endothelium and ADSC. In our experiments TNF-α pre-treatment of ADSC resulted in increased adhesion of THP-1 monocytes seeded over ADSC monolayer at both time points (40 and 120 min), which supported our data on increased ICAM-1 expression. Still when THP-1 were added to ADSC in their conditioned medium (after TNF-α treatment) we found adhesion to further increase compared to fresh medium.

We may speculate that conditioned medium contains a "cocktail" of pro-adhesive factors produced by TNF-α-treated ADSC. Positive mediators of monocyte adhesion may include chemokines known to promote monocyte activation, i.e. MCP-1 or IL-8, which were up-regulated in TNF-α-treated ADSC (Fig. 4C, D).

At the same time, adhesion of TNF-α-stimulated ADSC seeded on top of HUVEC monolayer was significantly decreased at 40 minutes (Fig. 3B). Still, at 120 min of incubation phase of spreading was not influenced by TNF-α suggesting that it has attenuated some factor(s) responsible only for initial phase of interaction between cells. These factors are to be identified in further studies and may be common with pericytes that share a number of proteoglycans (i.e., NG2).

In a triple adhesion experiment mixed suspension of ADSC and THP-1 was seeded over a HUVEC monolayer. Pre-treatment of ADSC with TNF-α resulted in decreased adhesion to endothelium, which was concordant with decline in THP-1 adhesion as well. This can be also attributed to increasing of ICAM-1 expression resulting in a stronger interaction between ADSC and monocytes. Putatively potent interaction between ADSC and THP-1 acted as a decoy drawing ADSC from adhering to HUVEC. Subsequently ADSC/THP-1 aggregates were washed from the culture imitating lower binding of ADSC to HUVEC (Fig. 3C).

Described effects of TNF-α on ADSC properties can be mediated by a number of signaling pathways triggered by TNF-α via its receptors. Taking into account our data on cell survival and ROS production PI3K/Akt/Rac1 axis was of particular interest for us.

It has been shown that PI3K/Akt signaling mediates angiogenesis [Jiang et al., 2000], and that PI3K/Akt/Rac1 pathway regulates cell survival, migration, invasion and ROS generation [Shin et al., 2008; Du et al., 2011]. Production of ROS can be mediated by Rac1, which is

a small GTPase inducing active NAD(P)H oxidase complex assembly [Hordijk, 2006]. The latter via ROS generation plays a central role in neovascularization and wound healing [Nijmeh et al., 2010]. Moreover, Rac1 is involved in regulation of cytoskeleton remodeling and F-actin microfibril formation [Chung et al., 2000].

We demonstrated that both Akt and Rac1(S71) were phosphorylated after ADSC stimulation by TNF-α. Our data indicated that ADSC migration is ROS-depending and cells generating ROS are localized on the edge of the healing "wound". Among ROS-generating enzymes NAD(P)H oxidase is a highly probable candidate especially taking into account Akt/Rac1(S71) phosphorylation found by western blot analysis. Still, generation of ROS by a number of cells under inflammatory conditions may have ambiguous effects. ROS can act as a potent inductor of tissue repair and infection eradication, but can also be involved in endothelial dysfunction and tumorogenesis [Alfadda and Sallam, 2012].

Downstream signaling activated by Akt may lead to induction of NF-κB [Dan et al., 2008] and Rac1 phosphorylation is known to further enhance this effect [Schwarz et al., 2012]. We analyzed NF-κB activation after TNF-α treatment by degradation of inhibitory protein, IκB. It is known that many of NF-κB target genes are regulators of angiogenesis. We have shown that the expression of some NF-κB-regulated angiogenic factors: (angiopoietin-1, FGF2, VEGF) and chemokines—MCP-1, IL-6 and IL-8 (Table II) were increased after TNF-α treatment. Inflammatory chemokines play a role in angiogenesis due to their ability to regulate activation of endothelial cells and attract monocytes to the injured area where they promote and orchestrate angiogenesis [Ito et al., 1997; Li et al., 2005].

Obtained data suggest that TNF-α shifts ADSC expression profile to a more angiogenic type. Still, this may also be described as a "trigger phenotype" with ADSC secreting strong mitogens (VEGF, FGF2) required to initiate vessel sprouting, but insufficient for vessel maturation. This speculation was in part supported by our finding that TNF-α down-regulates expression of TGF-β known to be essential for stabilization of de novo formed blood vessels and to induce differentiation of perimural cells into pericytes and smooth muscle cells [Hirschi et al., 1998; Choy and Derynck, 2003].

Still angiogenesis induced in presence of MSC results in establishment of a functional network of stable vessels and MSC may behave in a pericyte-like manner ensuring blood vessel stabilization [Merfeld-Clauss et al., 2010]. This prompted us to evaluate whether stimulation of ADSC with TNF-α may enhance their positive influence on vessel maturation.

In fibrin gel bead assay presence of TNF-α stimulated ADSC resulted in more active sprouts formation and branching of bead-attached HUVEC that led to formation of microvessel-like structures with a lumen by day 5 (Fig. 6 and S2). This enhancement of tubulogenesis can be attributed to observed increment of growth factor production by ADSC after TNF-α stimulation. Interestingly in absence of ADSC endothelial cells failed to form a network suggesting importance of paracrine factors produced by MSC.

It has been mentioned that by day 5 ADSC were aligning next to formed microtubules demonstrating pericyte-like behavior (Fig. 6C and S2B). This observation suggested that besides driving endothelial cells to form new vessels ADSC might possess a certain extent of pericyte function positioning adjacent to a de novo formed tube and enhancing vessel maturation. This partially confirmed our initial assumption that ADSC may launch angiogenesis via paracrine mechanism (which was enhanced by TNF-α) with a kind of "switch" to pericyte function after initial sprouting is complete. Peri-endothelial alignment of ADSC was independent of TNF-α treatment (observed in all specimen) and hard to quantify in our model, so our suggestion on ADSC function as pericytes are bound to certain limitations.

Generally, our data are consistent with the concept that MSC can be involved in both – initial and advanced stages of angiogenesis. Merfeld-Clause in their recent paper showed that ADSC even might acquire mural cell properties initiated by direct contact with endothelial cells [Merfeld-Clause et al., 2014]. Our data also indicated that inflammatory environment (imitated by TNF-α treatment) has a potentiating effect on pro-angiogenic characteristics of MSC and ADSC in particular. MCP-1 is one of the most important components of this inflammatory environment. It is well established that MCP-1 together with IL-8 are co-expressed during initial stages of wound healing [Salcedo et al., 2000] and both of them despite being described as inflammatory chemokines possess angiogenic properties. In case of IL-8 its role in TNF-α-mediated enhancement of angiogenic properties of ADSC was convincingly demonstrated by an elegant work by [Heo et al., 2011]. Meanwhile data related to contribution of MCP-1 to ADSC-induced angiogenesis are less abundant. It is known that CCR2 (surface receptor for MCP-1) is expressed on endothelial cells and MCP-1 can contribute to angiogenesis by induction of endothelial cell migration and sprouting in a number of models of angiogenesis [Salcedo et al., 2000]. Role of MCP-1 produced by ADSC was assessed by lentivirus-mediated MCP-1 silencing or treatment with Ingramon (interfering with binding of MCP-1 to heparin). We obtained similar data using both approaches and found that TNF-α effects were significantly reduced in MCP-1-silenced conditions. We found drastic decline of microvessels length in fibrin gel bead assay, but little effect on sprouts number was observed. These results suggested that increase of MCP-1 expression in ADSC caused by TNF-a may have a significant contribution to enhancement of their angiogenic properties.

Abovementioned changes of ADSC functions after TNF-α stimulation might result in enhanced angiogenic efficacy of these cells when administered to ischemic tissue. To address this assumption we turned to an in vivo model of hind limb ischemia in mice. Obtained results were consistent with data indicating increased angiogenic potential of TNF-α-treated ADSC. Indeed, treatment of ADSC with 5 ng/ml TNF-α prior to administration resulted in rapid blood flow recovery in the ischemic limb compared to untreated ADSC. Still, the difference was significant only at the initial steps of recovery (at day 7), but at day 14 after administration of cell suspensions, both groups (TNF-α and untreated cells) showed comparable perfusion values (Fig. 7C).

Histology data obtained in our study was consistent with in vitro changes induced by TNF-α, which can be described as "pro-angiogenic" and "pro-inflammatory" shift of ADSC secretome. Reduction of necrotic tissue area in skeletal muscle can be attributed

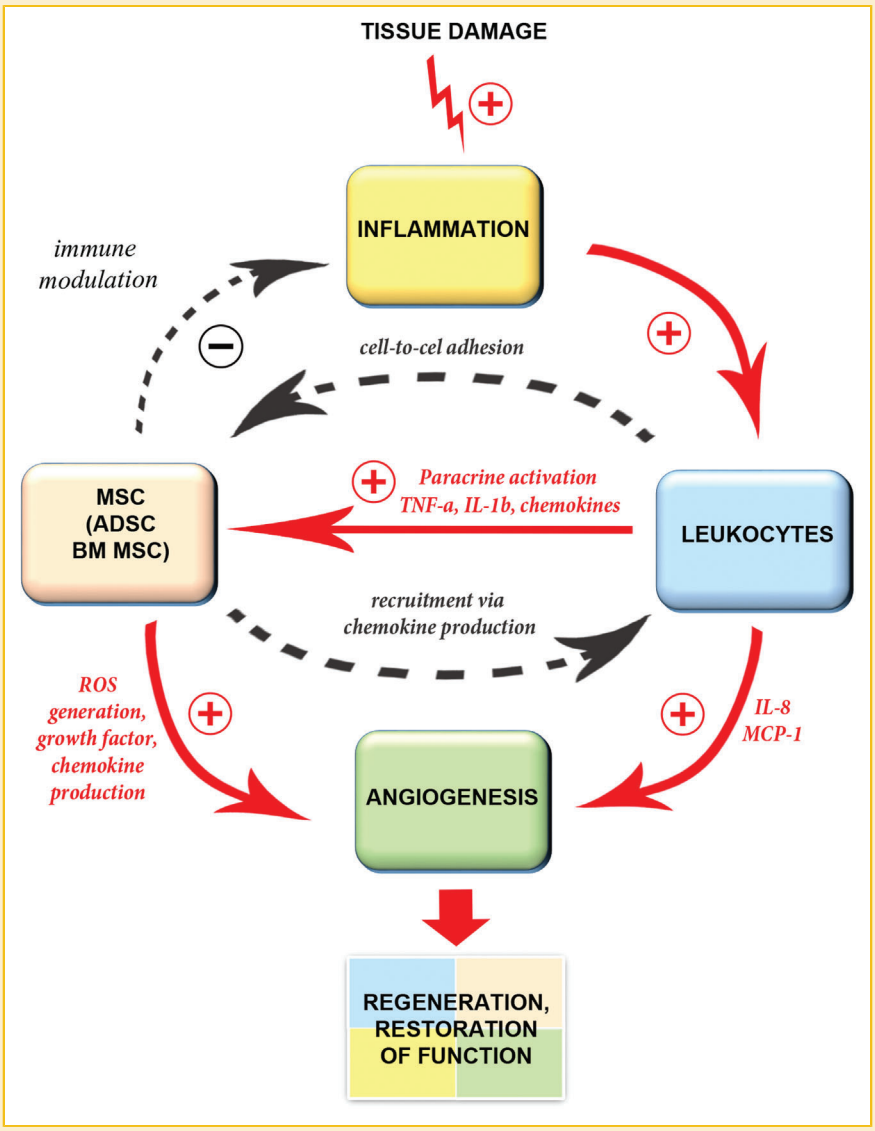

Fig. 8. General schematic representation of MSC potential for regeneration.

to effects of ADSC, which produce pro-survival cytokines favoring muscle fiber viability compared to untreated control (saline). Skeletal muscle injected with TNF-α-treated ADSC had the lowest necrosis span of all study groups, which can be mediated by up-regulation of VEGF165, FGF2 and other cytokines that stimulate survival. Infiltration of muscle by inflammatory cells was significantly reduced in ADSC-treated animals compared to saline, but we found that treatment by TNF-α totally abolish this effect. We may speculate that observed up-regulation of chemokines after TNF-α treatment can facilitate invasion of inflammatory cells from blood flow to ischemic muscles (Fig. 7B).

Vascular density assessment indicated enhancement of angiogenesis by day 14 in both groups of animals that received ADSC. Surprisingly CD31+ capillaries count in ADSC+TNF-α animals was significantly lower compared to ADSC. Still this finding did not undermine our suggestion about TNF-α stimulating effect on ADSC angiogenic potential as ADSC+TNF-α group had the highest count of α-SMA+ arterioles (Fig. S5 and Table III). These medium-caliber blood vessels contribute to limb perfusion greatly and may compensate interrupted blood supply to prevent muscle necrosis. Overall, we can speculate that vascular density assessment was concordant with Doppler data. ADSC group had the highest capillary counts in contrast to ADSC+TNF-α where arterioles played the major role in limb perfusion restoration, which resulted in comparable relative perfusion by day 14 (Fig. 7A, C). Possible mechanism for TNF-α-driven enhancement of arteriogenesis relies on a well-known role of MCP-1 in blood vessel remodeling and monocyte attraction, which is of crucial importance for arteriogenic response [Ito et al., 1997; van Amerongen et al., 2007].

Described study has certain sets of preliminary data and, thus, bound to limitations. For example, MCP-1 was one of the chemokines actively produced after stimulation by TNF-α and was shown in vitro to have significant contribution to effects of TNF-α-treated ADSC. Certainly, obtained results on arteriogenesis are not confined to effects of chemokines and MCP-1 in particular and can be attributed to a large repertoire of cytokines produced by stimulated ADSC. Overall, these results can be expanded to certain extent using transcriptome or proteome analysis, which may indicate families and clusters of proteins regulated by TNF-α in MSC.

Signaling activation by TNF-α may also have a number of alternative pathways to be screened yet we have focused on the ones, which control cell′s properties that play role in angiogenesis, proliferation and migration.

We also may be interested in graft retention analysis to evaluate survival of ADSC transplanted after TNF-α-treatment. TNF-α stimulated ADSC′s proliferation, production of pro-survival cytokines and activation of Akt pathway and this might have impact on therapeutic efficiency as more cells would be able to exert there effects surviving in inflammatory and hypoxic environment of ischemic tissue. Still, we omitted this test as far as our previously obtained data in the same model using ADSC expressing VEGF165 after viral transduction [Shevchenko et al., 2013] revealed no difference in graft retain. Still, these issues might be addressed in out further studies and give new data on cellular basis of ADSC therapeutic application.

Overall, we can estimate the role of MSC (and ADSC in particular) as a "big name" player in the cycle of tissue regeneration. In early stages of regeneration MSC are driven from their quiescent state by inflammatory stimuli (including TNF-α) to participate in leukocyte recruitment via increased production of chemokines. In later phases when resolution of inflammation commences MSCs are known to take part in modulation of immune response [Singer and Caplan, 2011] within tissue and lead the process to "exit" from the cycle, which can be presented schematically at Figure 8.

To conclude our study suggests that TNF-α enhances ADSC angiogenic potential and their regenerative abilities by stimulation of ADSC growth, expression of angiogenic factors and modulation of cell-to-cell interaction. Besides basic insights into MSC mode of action in natural environment it also provides certain clues on potential therapeutic application of this cell type, which gained significant interest in recent years.

ACKNOWLEDGMENTS

The authors thank Dr T. Krasnikova (Russian Cardiology Research and Production Centre, Moscow, Russia) for kindly providing us with Ingramon. Authors express gratitude to Dr. E. Gluhanyuk for his assistance during quantification of photomicrographs and to O. Grigorieva for assistance in ADSC isolation.

REFERENCES

Alfadda AA, Sallam RM. 2012. Reactive oxygen species in health and disease. J Biomed Biotechnol 2012:936486.

Arefieva TI, Krasnikova TL, Potekhina AV, Ruleva NU, Nikitin PI, Ksenevich TI, Gorshkov BG, Sidorova MV, Bespalova ZhD, Kukhtina NB, Provatorov SI, Noeva EA, Chazov EI. 2011. Synthetic peptide fragment (65-76) of monocyte chemotactic protein-1 (MCP-1) inhibits MCP-1 binding to heparin and possesses anti-inflammatory activity in stable angina patients after coronary stenting. Inflamm Res 60(10):955–964.

Azad GK, Tomar RS. 2014. Ebselen, a promising antioxidant drug: mechanisms of action and targets of biological pathways. Mol Biol Rep. 41(8):4865–4879.

Baek SJ, Kang SK, Ra JC. 2011. In vitro migration capacity of human adipose tissue-derived mesenchymal stem cells reflects their expression of receptors for chemokines and growth factors. Exp Mol Med. 43(10):596–603.

Bertassoli BM, de Assis Neto AC, de Oliveira FD, Machado Arroyo MA, Pires Ferrão JS, da Silva JB, Pignatari GC, Braga PB. 2013. Mesenchymal Stem Cells ? Emphasis in Adipose Tissue. Braz Arch Biol Technol 56(4):607–617.

Böcker W, Docheva D, Prall WC, Egea V, Pappou E, Rossmann O, Popov C, Mutschler W, Ries C, Schieker M. 2008. IKK-2 is required for TNF-alpha-induced invasion and proliferation of human mesenchymal stem cells. J Mol Med (Berl) 86(10):1183–1192.

Boutros T, Chevet E, Metrakos P. 2008. Mitogen-activated protein (MAP) kinase/MAPkinase phosphatase regulation: roles in cell growth, death, and cancer. Pharmacol Rev 60(3):261–310.

Bradley JR 2008. TNF-mediated inflammatory disease. J Pathol 214(2):149–160.

Choy L, Derynck R T. 2003. Transforming growth factor-beta inhibits adipocyte differentiation by Smad3 interacting with CCAAT/enhancer-binding protein (C/EBP) and repressing C/EBP transactivation function. J Biol Chem 278(11):9609–9619.

Chung CY, Lee S, Briscoe C, Ellsworth C, Firtel RA. 2000. Role of Rac in controlling the actin cytoskeleton and chemotaxis in motile cells. Proc Natl Acad Sci USA 97(10):5225–5230.

Corredor J, Yan F, Shen CC, Tong W, John SK, Wilson G, Whitehead R, Polk DB. 2003. Tumor necrosis factor regulates intestinal epithelial cell migration by receptor-dependent mechanisms. Am J Physiol Cell Physiol 284(4):C953–C961.

Coussens LM, Werb Z. 2002. Inflammation and cancer. Nature 420-(6917):860–867.

Crisostomo PR, Wang Y, Markel TA, Wang M, Lahm T, Meldrum DR. 2008. Human mesenchymal stem cells stimulated by TNF-alpha, LPS, or hypoxia produce growth factors by an NF kappa B- but not JNK-dependent mechanism. Am J Physiol Cell Physiol 294(3):C675–C682.

da Silva Meirelles L, Chagastelles PC, Nardi NB. 2006. Mesenchymal stem cells reside in virtually all post-natal organs and tissues. J Cell Sci 119:2204–2213.

Dan HC, Cooper MJ, Cogswell PC, Duncan JA, Ting JP, Baldwin AS. 2008. Akt-dependent regulation of NFκB is controlled by mTOR and Raptor in association with IKK. Genes Dev 22:1490–1500.

Du J, Xu R, Hu Z, Tian Y, Zhu Y, Gu L, Zhou L. 2011. PI3K and ERK-induced Rac1 activation mediates hypoxia-induced HIF-1α expression in MCF-7 breast cancer cells. PLoS ONE 6(9):e25213.

Heo SC, Jeon ES, Lee IH, Kim HS, Kim MB, Kim JH. 2011. Tumor necrosis factor-α-activated human adipose tissue-derived mesenchymal stem cells accelerate cutaneous wound healing through paracrine mechanisms. J Invest Dermatol 131(7):1559–1567.

Hirschi KK, Rohovsky SA, D′Amore PA. 1998. PDGF, TGF-beta, and heterotypic cell-cell interactions mediate endothelial cell-induced recruitment of 10T1/2 cells and their differentiation to a smooth muscle fate. J Cell Biol 141(3):805–814.

Hordijk PL. 2006. Regulation of NADPH oxidases: the role of Rac proteins. Circ Res 98(4):453–462.

Ikeda S, Yamaoka-Tojo M, Hilenski L, Patrushev NA, Anwar GM, Quinn MT, Ushio-Fukai M. 2005. IQGAP1 regulates reactive oxygen species-dependent endothelial cell migration through interacting with Nox2. Arterioscler Thromb Vasc Biol 25(11):2295–2300.

Ito WD, Arras M, Winkler B, Scholz D, Schaper J, Schaper W. 1997. Monocyte chemotacticprotein-1 increases collateral and peripheral conductance after femoral artery occlusion. Circ Res 80(6):829–837.

Jiang BH, Zheng JZ, Aoki M, Vogt PK. 2000. Phosphatidylinositol 3-kinase signaling mediates angiogenesis and expression of vascular endothelial growth factor in endothelial cells. Proc Natl Acad Sci USA 97(4):1749–1753.

Jones DL, Wagers AJ. 2008. No place like home: anatomy and function of the stem cell niche. Nat Rev Mol Cell Biol 9(1):11–21.

Kwon T, Kwon DY, Chun J, Kim JH, Kang SS. 2000. Akt protein kinase inhibits Rac1-GTP binding through phosphorylation at serine 71 of Rac1. J Biol Chem 275(1):423–428.

Lai Y, Shen Y, Liu XH, Zhang Y, Zeng Y, Liu YF. 2011. Interleukin-8 induces the endothelial cell migration through the activation of phosphoinositide 3-kinase-Rac1/RhoA pathway. Int J Biol Sci 7(6):782–791.

Lee MJ, Kim J, Kim MY, Bae Y-S, Ryn SH, Lee TG, Kim JH. 2010. Proteomic analysis of tumor necrosis factor-α-induced secretome of human adipose tissue-derived mesenchymal stem cells. J Proteomic Res 9:1752–1762.

Li A, Varney ML, Valasek J, Godfrey M, Dave BJ, Singh RK. 2005. Autocrine role of interleukin-8 in induction of endothelial cell proliferation, survival, migration and MMP-2 production and angiogenesis. Angiogenesis 8(1):63–71.

Long EO. 2011. ICAM-1: getting a grip on leukocyte adhesion. J Immunol 186(9):5021–5023.

Low-Marchelli JM, Ardi VC, Vizcarra EA, van Rooijen N, Quigley JP, Yang J. 2013. Twist1 induces CCL2 and recruits macrophages to promote angiogenesis. Cancer Res 73(2):662–671.

Makarevich P, Tsokolaeva Z, Shevelev A, Rybalkin I, Shevchenko E, Beloglazova I, Vlasik T, Tkachuk V, Parfyonova Y. 2012. Combined transfer of human VEGF165 and HGF genes renders potent angiogenic effect in ischemic skeletal muscle. PLoS One 7(6):e38776.

Medvedev AE, Espevik T, Ranges G, Sundan A. 1996. Distinct roles of the two tumor necrosis factor (TNF) receptors in modulating TNF and lymphotoxin alpha effects. J Biol Chem 271(16):9778–9784.

Menshikov M, Torosyan N, Elizarova E, Plakida K, Vorotnikov A, Parfyonova Y, Stepanova V, Bobik A, Berk B, Tkachuk V. 2006. Urokinase induces matrix metalloproteinase-9/gelatinase B expression in THP-1 monocytes via ERK1/2 and cytosolic phospholipase A2 activation and eicosanoid production. J Vasc Res 43:482–490.

Merfeld-Clauss S, Gollahalli N, March KL, Traktuev DO. 2010. Adipose tissue progenitor cells directly interact with endothelial cells to induce vascular network formation. Tissue Eng Part A 16(9):2953–2966.

Merfeld-Clauss S, Lupov IP, Lu H, Feng D, Compton-Craig P, March KL, Traktuev DO. 2014. Adipose stromal cells differentiate along a smooth muscle lineage pathway upon endothelial cell contact via induction of activin A. Circ Res 115(9):800–809.

Moon SK, Cha BY, Kim CH. 2004. ERK1/2 mediates TNF-alpha-induced matrix metalloproteinase-9 expression in human vascular smooth muscle cells via the regulation of NF-kappaB and AP-1: Involvement of the ras dependent pathway. J Cell Physiol 198(3):417–427.

Möpert K, Löffler K, Röder N, Kaufmann J, Santel A. 2012. Depletion of protein kinase N3 (PKN3) impairs actin and adherens junctions dynamics and attenuates endothelial cell activation. Eur J Cell Biol 91(9):694–705.

Mosmann T 1983. Rapid colorimetric assay for cellular growth and survival: application to proliferation and cytotoxicity assays. J Immunol Methods 65:55–63.

Naudé PJ, den Boer JA, Luiten PG, Eisel UL. 2011. Tumor necrosis factor receptor cross-talk. FEBS J 278(6):888–898.

Nesselmann C, Ma N, Bieback K, Wagner W, Ho A, Konttinen YT, Zwang H, Hinescu ME, Steinkoff G. 2008. Mesenchimal stem cells and cardiac repair. J Cell Mol Med 12(58):1795–1810.

Nijmeh J, Moldobaeva A, Wagner EM. 2010. Role of ROS in ischemia-induced lung angiogenesis. Am J Physiol Lung Cell Mol Physiol 299(4):L535–L541.

Niu J, Azfer A, Zhelyabovska O, Fatma S, Kolattukudy PE. 2008. Monocyte chemotactic protein (MCP)-1 promotes angiogenesis via a novel transcription factor, MCP-1-induced protein (MCPIP). J Biol Chem 283(21):14542–14551.

Ozes ON, Mayo LD, Gustin JA, Pfeffer SR, Pfeffer LM, Donner DB. 1999. NF-kappaB activation by tumour necrosis factor requires the Akt serine-threonine kinase. Nature 401(6748):82–85.

Puls A, Eliopoulos AG, Nobes CD, Bridges T, Young LS, Hall A. 1999. Activation of the small GTPase Cdc42 by the inflammatory cytokines TNF (alpha) and IL-1, and by the Epstein-Barr virus transforming protein LMP1. J Cell Sci 112:2983–2992.

Rohringer S, Hofbauer P, Schneider KH, Husa AM, Feichtinger G, Peterbauer-Scherb A, Redl H, Holnthoner W. 2014. Mechanisms of vasculogenesis in 3D fibrin matrices mediated by the interaction of adipose-derived stem cells and endothelial cells. Angiogenesis 17(4):921–933.

Salcedo R, Ponce ML, Young HA, Wasserman K, Ward JM, Kleinman HK, Oppenheim JJ, Murphy WJ. 2000. Human endothelial cells express CCR2 and respond to MCP-1: direct role of MCP-1 in angiogenesis and tumor progression. Blood 96(1):34–40.

Schoentaube J, Olling A, Tatge H, Just I, Gerhard R. 2009. Serine-71 phosphorylation of Rac1/Cdc42 diminishes the pathogenic effect of Clostridium difficile toxin A. Cell Microbiol 11(12):1816–1826.

Schwarz J, Proff J, Hävemeier A, Ladwein M, Rottner K, Barlag B, Pich A, Tatge H, Just I, Gerhard R. 2012. Serine-71 phosphorylation of Rac1 modulates downstream signaling. PLoS One 7(9):e44358.

Shevchenko EK, Makarevich PI, Tsokolaeva ZI, Boldyreva MA, Sysoeva VY, Tkachuk VA, Parfyonova YV. 2013. Transplantation of modified human adipose derived stromal cells expressing VEGF165 results in more efficient angiogenic response in ischemic skeletal muscle. J Transl Med 6(11):138.

Shi Y, Xia YY, Wang L, Liu R, Khoo KS, Feng ZW. 2012. Neural cell adhesion molecule modulates mesenchymal stromal cell migration via activation of MAPK/ERK signaling. Exp Cell Res 318(17):2257–2267.

Shin DH, Kim OH, Jun HS, Kang MK. 2008. Inhibitory effect of capsaicin on B16-F10 melanoma cell migration via the phosphatidylinositol 3-kinase/Akt/Rac1 signal pathway. Exp Mol Med 40(5):486–494.

Singer AJ, Clark RA. 1999. Cutaneous wound healing. N Engl J Med 341(10):738–746.

Singer NG, Caplan AI. 2011. Mesenchymal stem cells: mechanisms of inflammation. Annu Rev Pathol 6:457–478.

van Amerongen MJ, Harmsen MC, van Rooijen N, Petersen AH, van Luyn MJ. 2007. Macrophage depletion impairs wound healing and increases left ventricular remodeling after myocardial injury in mice. Am J Pathol 170(3):818–829.

Xiao Q, Wang SK, Tian H, Xin L, Zou ZG, Hu YL, Chang CM, Wang XY, Yin QS, Zhang XH, Wang LY. 2012. TNF-α increases bone marrow mesenchymal stem cell migration to ischemic tissues. Cell Biochem Biophys 62(3):409–414.

Zubkova ES, Makarevich PI, Parfyonova YV, Menshikov MYu, Semenkova LN, Dudich IV, Dudich EI, Khromykh LM. 2012. Recombinant human alpha-fetoprotein as a regulator of adipose tissue stromal cell activity. Bioorg Khim 38(5):524–534.

SUPPORTING INFORMATION

Additional supporting information may be found in the online version of this article at the publisher's web-site.